https://doi.org/10.5194/egusphere-2026-2843
Preprint. Discussion started: 25 August 2026

Potential of common extraction procedures to evaluate organic carbon association with different species of metal(loid)s in soils

Bright E. Amenkhienan, Feike A. Dijkstra, Charles Warren, and Balwant Singh.

School of Life and Environmental Sciences, The University of Sydney, New South Wales, 2015, Australia.

Correspondence to: bright.amenkhienan@sydney.edu.au

Abstract

A strong association of organic carbon (OC) with metal oxides, especially iron (Fe) and aluminium (Al) oxides has been reported in several studies. However, the role of various species of Fe, Al, manganese (Mn) and silicon (Si) in the stabilisation of OC in Fe-rich and phosphorus (P) deficient soils, common in tropical and sub-tropical regions, remains poorly understood. To address this, we collected topsoil (0-20 cm) and subsoil (20-40 cm) samples from 37 sites across agricultural regions of New South Wales, Australia. Soil samples were subjected to three separate chemical extractions, i.e., sodium pyrophosphate (PP) to extract organo-metal complexes, ammonium oxalate (OX) to extract poorly crystalline and short-range order (SRO) minerals and dithionite citrate bicarbonate (DCB) to extract total metal oxides, to determine OC associated with each of the extractions. Soil organic carbon (SOC) was extracted in the sequence: C_{PP}>C_{DCB}>C_{OX}, with a mean of 62±0.16 %, 41±0.19 % and 28±0.21 %, respectively, of the total C extracted from soils. The extraction sequence for Fe was: Fe_{DCB}>Fe_{OX}>Fe_{PP}, with a mean of 49±0.18 %, 9±0.05 % and 3±0.03 %, respectively, of the total Fe extracted from soils. Aluminium was extracted in the same sequence as Fe, with a mean value of 4.0±0.02 % for Al_{DCB}, 3.9±0.02 % for Al_{OX} and 2.0±0.01 % for Al_{PP} of the total Al. Manganese extraction occurred in the sequence - Mn_{OX}>Mn_{DCB}>Mn_{PP}, with an average of 78±1.58 %, 65±1.10 % and 43±1.23 %, respectively, of the total Mn extracted. All extractants dissolved <1 % of the total Si. All extractable forms of Fe and Al showed significant positive correlations with extractable C, which suggested their potential role in the preservation of SOC. The large fraction of OC extracted by PP suggested that organic-Fe/Al complexes constituted a large fraction of the total SOC in the studied soils. The significant amount of OC associated with OX extraction also indicated that a substantial portion of the SOC was associated with SRO and poorly crystalline Fe oxides, while a relatively small proportion of the total OC was extracted by DCB suggested a limited role of crystalline Fe/Al oxides in the OC stabilisation.

1 Introduction

A huge amount (~2200 Pg) of organic carbon (OC) in the terrestrial ecosystems is stored in the top 100 cm soil, which is more than the combined together in the atmosphere and vegetation (Batjes, 2014). Soil OC carbon plays a key role in providing multiple ecosystem services including plant production, nutrient cycling, water storage and purification, and climate regulation (Ontl and Schulte, 2012; Paul, 2016; Jackson et al., 2017). Soil OC is an important and significant component of the global C biogeochemical cycle of C and a small change in the SOC pool can substantially increase or decrease atmospheric CO_2 concentration, thus has a

https://doi.org/10.5194/egusphere-2026-2843
Preprint. Discussion started: 25 August 2026

potential to accelerate or mitigate global warming (Lal et al., 1999; Lal, 2004; Crowther et al., 2016). Managing soils to boost OC stocks has been suggested as a strategy to reduce the rise in atmospheric CO_2 concentration (Mikutta et al., 2006). The association of OC with minerals has received significant attention in recent decades, because it is recognised as a key mechanism in the stabilisation and long-term storage of OC in soils (Sollins et al., 1996; Torn et al., 1997; Lützow et al., 2006; Kögel-Knabner et al., 2008; Kleber et al., 2015; Lehmann and Kleber, 2015). Several mechanisms, including surface complexation, cation bridging, weak chemical interactions and co-precipitation, have been postulated in the formation of mineral-associated organic matter (MAOM) in soils (Kögel-Knabner et al., 2008; von Lützow et al., 2008; Kleber et al., 2015). Chemical interactions of OC with minerals decrease its susceptibility towards oxidative attack and microbial mineralisation, which subsequently results in the stabilisation and accumulation of OC in soils (Kaiser and Guggenberger, 2003; Kalbitz et al., 2005; Kögel-Knabner et al., 2008). The nature of association and stability of the MAOM in different soil types are still not well understood.

Iron (Fe) and aluminium (Al) are among the most prevalent elements in soils (Cornell and Schwertmann, 2003). Iron and Al oxides (the term 'oxides' used for brevity, it includes hydroxides, oxyhydroxides and oxides) are formed in soils from the weathering and dissolution of primary minerals (Chadwick and Chorover, 2001). These minerals are effective sorbents for dissolved OC because of their high specific surface area (SSA) and abundant reactive surfaces (Kaiser and Guggenberger, 2000). Iron bound C has been estimated to contribute 15 to 78 % of the total OC in sediments and soils (Cornell and Schwertmann, 2003; Wagai and Mayer, 2007; Zhao et al., 2016; Kramer and Chadwick, 2018). The concentration of Fe and Al oxides is generally high in intensively weathered soils of tropical and subtropical regions (Singh and Gilkes, 1992; Mikutta et al., 2009). The surface hydroxyl groups of Fe oxides are capable of interacting with carboxyl or hydroxamate groups of SOC via ligand exchange, thus stabilise and protect SOC against microbial mineralisation (Gu et al., 1994; Mikutta et al., 2007; Kleber et al., 2015; Chen et al., 2020). Chemical reactions between Fe oxides and organic functional groups have been well studied and it has been found that Fe oxides preferentially bind with aromatic and carboxylic functional groups of OC (Gu et al., 1994; Kaiser, 2003; Chen et al., 2014; Yeasmin et al., 2014). Co-precipitation of dissolved OC with polyvalent cations, such as Fe and Al, in organo-metal complexes also stabilises SOC (Baldock and Skjemstad, 2000; Scheel et al., 2007; Eusterhues et al., 2011; Mikutta et al., 2014). Co-precipitation may occur due to changes in soil pH or redox conditions (Wagai and Mayer, 2007; Fritzsche et al., 2015). For example, in temporarily waterlogged paddy soils, upon aeration, dissolved Fe (II) is rapidly oxidised to relatively insoluble Fe (III) and large amount of OC co-precipitate with Fe (Chen et al., 2014; Song et al., 2022). Some studies have reported that co-precipitation (organo-metal complexes) was more effective in sequestering dissolved OC than adsorption (Mikutta et al., 2011; Chen et al., 2014; Mikutta et al., 2014). Despite the wide-spread occurrence of Fe oxides in Australian soils, the association of OC with Fe oxides remains poorly understood in these soils (Davey et al., 1975; Singh and Gilkes, 1992; Viscarra Rossel et al., 2010).

Manganese (Mn) is a redox-active element that can strongly interact with organic functional groups, thus influencing the stabilisation of SOC (Li et al., 2021). Relative to its bulk soil concentration, Mn oxides could be strongly enriched in OC (Rennert et al., 2014). The poorly crystalline Mn oxides in particular possess relatively large SSA and high adsorption capacity for organics (Estes et al., 2017; Stuckey et al., 2018; Li et al., 2021), thereby stabilising and protecting OC against decomposition (Li et al., 2021). Mn oxides have several properties similar to Fe oxides (Li et al., 2021), except the point of zero charge, but the association of OC

https://doi.org/10.5194/egusphere-2026-2843
Preprint. Discussion started: 25 August 2026

with different forms of Mn in natural soils is rarely studied. Silicon (Si) plays a significant role in regulating the biogeochemical C cycle and stabilization of SOC. In the terrestrial ecosystem, the behaviour of Fe and Al may be regulated by biogeochemical cycling of Si through the formation of stable Fe-Si and Al-Si complexes (Pokrovski et al., 2003; Matus et al., 2014). Consequently, Si may play a significant role in stabilising SOC (Song et al., 2018), either directly by stabilisation of SOC by chemical interaction with amorphous Si (phytolith) or indirectly by MAOM stabilisation and soil aggregation (Pokrovski et al., 2003; Matus et al., 2014; Zhang et al., 2016).

The abundance of various forms of Fe, Al, Mn, and Si and reactive mineral phases in soils is frequently estimated by chemical extraction procedures. Extraction procedures using sodium pyrophosphate (PP), ammonium oxalate (OX), and dithionite-citrate-bicarbonate (DCB) reagents target certain metal phases (Mehra and Jackson, 1960; McKeague, 1967). Extraction methods are feasible, especially with large number of samples and can be easily adopted by commercial laboratories. In addition, these procedures are less-time consuming economical than spectroscopic and other methods (Rennert, 2019) and do not require specialised equipment. However, there are some potential pitfalls in the extraction methods, such as exclusive selectivity, interpretation of extracted phases and extraction efficiency, which may vary with soil properties (Parfitt and Childs, 1988; Kaiser and Zech, 1996; Pansu and Gautheyrou, 2006; Rennert, 2019; Voelz et al., 2019; Rennert and Lenhardt, 2025). Despite these drawbacks, extraction procedures offer the best option for the broad scale assessment of OC stabilisation with different forms of Fe, Al, Mn, and Si in soils. Other techniques, such as, X-ray diffraction and vibrational spectroscopy, are unable to distinguish the association of OC with different species of Fe and Al oxides (Coward et al., 2017). Numerous studies have used extraction procedure data to understand the stabilisation of SOC with Fe and Al oxides in relatively young soils from temperate soils (Kaiser and Guggenberger, 2000; Kleber et al., 2005; Wiseman and Püttmann, 2006; Kaiser et al., 2007; Wagai and Mayer, 2007; Rasmussen et al., 2018; Ashida et al., 2021), and in highly weathered soils (Coward et al., 2017; Wagai et al., 2020; Ye et al., 2022). Significant positive relationships between SOC and OX extractable Fe and Al highlight the important role of poorly crystalline Fe/Al oxides and/or short range order (SRO) Fe/Al oxides in the formation of MAOM in both surface (Rasmussen et al., 2006) and sub-surface soils (Kaiser and Guggenberger, 2000; Kleber et al., 2005; von Fromm et al., 2025). Likewise, crystalline Fe oxides content has been reported to be the major driver of MAOM abundance in soils and close relationships between DCB extractable Fe/Al and SOC content have been reported in soils from different regions (Mu et al., 2016; Zhao et al., 2016; Yu et al., 2019; Zhao et al., 2023). Many other studies have reported a significant relationship between PP extractable Fe/Al and SOC content in a wide range of soils, suggesting the relevance of organo-metal complexes in the stabilisation of SOC (Percival et al., 2000; Wagai and Mayer, 2007; Wagai et al., 2013; Lawrence et al., 2015; Hall and Thompson, 2022; Yu et al., 2023). Most of the published studies have evaluated relationships between different forms of extractable metals and SOC contents but did not actually quantify the OC content associated with different forms of extractable metal(loid)s. Wagai and Mayer (2007) determined OC associated with Fe oxides using dithionite-HCl extraction in several soils and estimated between 2 % and 25% of the total SOM was bound with Fe oxides. Heckmann et al (2018) used a selective and sequential procedure to evaluate OC association with different forms of Al and Fe in four soils and found the order: Na-pyrophosphate < hydroxylamine < dithionite-HCl. Thus, the largest pool of stabilized OC was found in organo-metal complexes that was extracted by Na-pyrophosphate. In this study, we have attempted to determine the

https://doi.org/10.5194/egusphere-2026-2843
Preprint. Discussion started: 25 August 2026

role of different species of Fe, Al, Mn and Si in the stabilisation of OC of P deficient and Fe-rich soils that occupy much of the tropic and subtropics and southern hemisphere including Australia. We have employed the most common chemical extraction procedures, acknowledging and accounting for possible errors involved in these, to evaluate the role of different metal(loid)s in OC stabilisation.

We used PP (pH 10), OX (pH 3) and DCB to extract organo-metal complexes, SRO and/or poorly crystalline metal phases and crystalline or free metal oxides, respectively, from a range of soil types with a wide range of Fe concentrations. Also, we used both top and sub-soils for this study. Soil OC associated with each of the extractable form was determined by analysing the residues after each extraction. The main aim was to quantitatively estimate the role of different fractions (or species) of metal(loid)s in stabilising OC in top- and sub-soils of agricultural regions of New South Wales, Australia. We hypothesised that poorly crystalline and SRO minerals of Fe, Al, Mn and Si contribute more to the stabilisation of OC in both top- and sub-soils. We further hypothesised that the concentration of Fe will be highest in soils and thus Fe will have the most prominent role in OC stabilisation amongst the metal(loid)s in both top- and sub-soils.

2. Materials and methods

2.1 Soil samples and handling

Topsoil (0 – 20 cm) and subsoil (20 – 40 cm) samples were collected from 37 locations across New South Wales, Australia (Fig. 1). The location names, coordinates, and Australian Soil Classification (ASC) of the soil samples are presented in Table S1. Soil samples were air-dried, crushed, passed through a 2 mm sieve and stored at room temperature for laboratory analysis. The dataset of the extractable metal(loid)s and C used for this study is presented in Table A1 and A2, respectively.

2.2 Soil physical and chemical properties

Soil pH and electrical conductivity (EC) were measured in 1:5 of soil and water extracts using a combined glass electrode pH meter and an EC meter, respectively (Rayment and Lyons, 2011). Particle size analysis (PSA) was determined by the hydrometer method (Gee and Or, 2002). Cation exchange capacity (CEC) was determined by the silver thiourea method (Rayment and Lyons, 2011). Total C and nitrogen (TN) were analysed using vario MACRO cube Elementar CHN analyser. Total Fe, Al, Mn, and Si were analysed using a PANalytical Minipal 4 X-Ray Florescence (XRF) spectrometer.

https://doi.org/10.5194/egusphere-2026-2843
Preprint. Discussion started: 25 August 2026

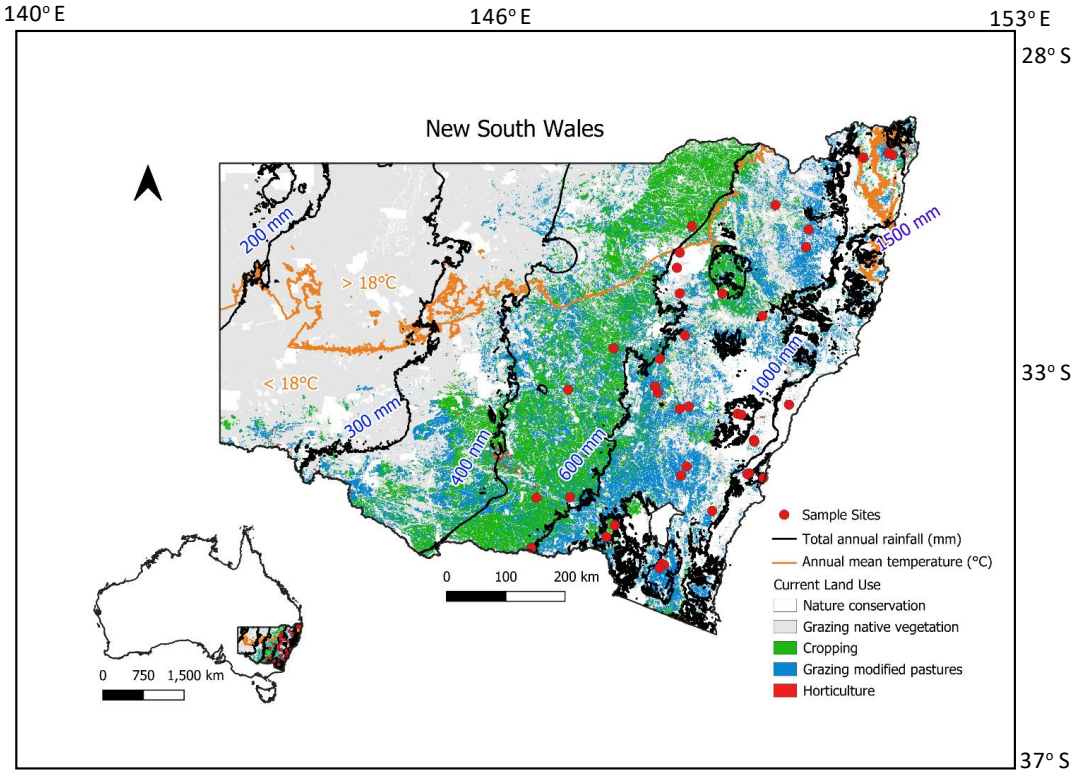

Figure 1. Map of New South Wales showing sampling (red dots) locations of soil samples, current land use, total annual rainfall and annual mean temperature.

2.3 Selective extraction procedure and analyses

Soil samples were subjected to three separate chemical extractions to dissolve different Fe phases (Table 1). Aluminium, Mn and Si were also measured in these extractions, however, the extractants are known to be most specific to Fe phases. All soil samples (in duplicates) were separately extracted by sodium pyrophosphate (PP, pH 10), ammonium oxalate (OX, pH 3), and dithionite-citrate-bicarbonate (DCB). To validate the quantification of extracted C, a subset of 10 samples (with a wide range in Fe content) were also extracted by sodium pyrophosphate (PP, pH 7.5), dithionite-hydrochloric acid (DH) and hydrochloric acid-hydroxylamine (HH), as described in more detail in Section 2.4. The concentrations of Fe, Al, Si and Mn in supernatants from all extractions were analysed using PerkinElmer Nexion 300x inductively coupled plasma-mass spectrometer (ICP-MS). The residues after each extraction were analysed for total C to determine OC extracted by each reagent.

https://doi.org/10.5194/egusphere-2026-2843
Preprint. Discussion started: 25 August 2026

Table 1. A summary of chemical extraction procedures and targeted phases.

Solvent	Concentration	Solvent pH	Target phases	Number of soil samples
Sodium pyrophosphate (PP)	0.1 M	10	Organic matter- complexed metals	74
Sodium pyrophosphate (PP)	0.1 M	7.5	Organic matter- complexed metals	10
Ammonium oxalate (OX)	0.2 M	3	Non-crystalline, amorphous, short-range-ordered (SRO) minerals and poorly crystalline minerals	74
Dithionite-citrate-bicarbonate (DCB)	0.3M, 1 M	8	Total 'free' oxides or pedogenic or crystalline metal oxides	74
Dithionite-Hydrochloric acid (DH)	0.05 M, 0.05 M	2.3	Total 'free' oxides or pedogenic phases or crystalline metal oxides	10
Hydrochloric acid-hydroxylamine (HH)	0.25 M 0.25 M	0.8	Non-crystalline, amorphous, short-range-ordered (SRO) minerals and poorly crystalline minerals	10

2.3.1 Sodium pyrophosphate (PP) at pH 10

Pyrophosphate extraction provides an estimate organic complexed or bound Fe and Al in soils (Loveland and Digby, 1984). We used the procedure described by McKeague (1967) to extract organic C complexed with Fe and Al, where 500 mg of soil was mixed with 50 ml of 0.1 M PP solution (pH 10) in 55 ml centrifuge tubes. The samples were shaken for 16 hours and centrifuged at 3280 × *g* and the supernatants filtered through a 0.2 µm PES membrane syringe filter (Merck Millipore, Millex-GP, 33 mm diameter) for ICP-MS analysis.

2.3.2 Acid ammonium oxalate (OX)

Extraction with 0.2 M ammonium oxalate (pH 3.0) in the dark dissolves SRO and poorly crystalline minerals (Schwertmann, 1964). For this extraction, 500 mg of soil was mixed with 30 ml of 0.2 M ammonium oxalate (pH 3.0) in 55 ml centrifuge tubes, and the mixture was shaken for 4 hours in the dark (Mckeague and Day, 1966). The suspensions were then centrifuged at 3280 × *g* for 10 minutes. The supernatants were filtered through a 0.2 µm PES membrane syringe filter for ICP-MS analysis.

2.3.3 Dithionite-citrate-bicarbonate (DCB)

Dithionite-citrate-bicarbonate extraction was used to extract pedogenic Fe and Al phases in soils (Mehra and Jackson, 1960). Briefly, 1 g of soil was mixed with 40 ml of 0.3 M sodium (Na)-citrate and 5 ml of 1 M Na-bicarbonate, in 55 ml centrifuge tubes. The tubes were heated in a water bath to 80°C for 10 min, then 1 g of sodium dithionite was added and stirred immediately for 1 min and then occasionally 5 min. After the digestion, 10 mL of saturated

https://doi.org/10.5194/egusphere-2026-2843
Preprint. Discussion started: 25 August 2026

sodium chloride (NaCl) solution was added to promote flocculation. The samples were centrifuged at 3280 × *g*, and the supernatants were filtered through Whatman 42 filter paper for the analysis. The extraction procedure was repeated twice for some of the soil samples, where brown or red colouration was observed.

2.4 Extractable C methodology validation

Two of the extraction procedures involve C containing reagents (i.e., oxalate in OX, and citrate and bicarbonate in DCB), hence we compared the residual total C in soils after OX and DCB extractions with comparable procedures, i.e. HH and DH, respectively, which do not employ C compounds in the extraction procedure (Heckman et al., 2018).

2.4.1 Sodium pyrophosphate (PP) at pH 7.5

Selective samples (with a range of total Fe content) were extracted with PP at pH 7.5 in duplicate to determine the peptization of Fe oxides at pH 10 (Parfitt and Childs, 1988; Rennert, 2019). The procedure of McKeague (1967) as described earlier was followed, except the PP solution pH was adjusted to 7.5 with hydrochloric acid (HCl). Selective samples containing a range of PP extractable Fe were used in the extraction.

2.4.2 Hydrochloric acid-hydroxylamine (HH)

Inorganic HH extraction targets SRO and/or amorphous Fe and Al oxides (Chao and Zhou, 1983; Ross et al., 1985). Acidified hydroxylamine is capable of extracting Fe phases (Chao and Zhou, 1983) that closely align with SRO minerals extraction procedure using acid ammonium oxalate (McKeague and Day, 1966). Acidified hydroxylamine is a C-free alternative to OX and the residual soil C analysis after this extraction was used to compare with the OX extractant soil residues. For this extraction, we weighed 500 mg soil into a 55 mL centrifuge tube, mixed with 30 ml of HH solution, the mixture was shaken for 16 hours and then centrifuged at 3280 × *g*. The supernatant was filtered through a 0.2 µm PES membrane syringe filter for ICP-MS analysis.

2.4.3 Dithionite-hydrochloric acid (DH)

Dithionite-hydrochloric acid is a C-free alternative to DCB to extract pedogenic Fe and Al phases just like DCB (Wagai and Mayer, 2007; Wagai et al., 2013). This extraction was performed on selective samples to compare the DH extractable C values to DCB extractable C values. 500 mg of soil was mixed with 30 ml of 57.4 mM sodium dithionite, shaken for 16 hours and centrifuged at 3280 × *g* for 40 mins. The supernatants were filtered through a 0.2 µm PES membrane syringe filter into another 50 ml centrifuge tubes. Soil residues were added with 10 ml of 0.05 M HCl, shaken for 1 hour and then centrifuged again. The supernatants were filtered as before and combined with Na dithionite extracts.

2.5 Post-extraction procedure and analysis

The soil residues after extractions were washed twice with ultrapure water to remove entrained solutions, centrifuged, dried overnight at 60 °C, lightly ground manually and weighed for total C analysis. Total C concentrations of the soil samples before and after extraction were analysed in duplicates using a vario MACRO cube Elementar CHN analyser. Total C concentration represents OC concentration because most of studied soils had acidic

https://doi.org/10.5194/egusphere-2026-2843
Preprint. Discussion started: 25 August 2026

pH values. The presence of carbonate was also tested by adding hydrochloric acid to soil samples with near neutral pH values.

2.6 Data Analysis

Paired t-test was used to determine differences in the concentrations of extractable metal(loid)s (Fe, Al, Mn and Si) and extractable C between samples from the two depths. Correlations between physical and chemical properties of soils were performed using Spearman's rho correlation. The generalised linear mixed model (GLMM) regression was used to determine relationships between extractable metal concentrations and other soil properties. In GLMM regression, we used extractable metal concentrations and soil properties as the fixed effects and soil types as the random effects. After running the model with all soil properties first, the non-significant variables were removed from the fixed effects, and the model was re-run to obtain variables that were significant in the model. For data analysis, we used JMP Pro software (Version 17.0, SAS Institute Incorporation, Cary, NC, USA).

3 Results

3.1. Soil physical and chemical characteristics

A summary of soil physical and chemical properties is presented in Table 2. Soil pH was strongly acidic to near neutral, with values ranging from 4.7 to 7.6. The electrical conductivity (EC) values of soils were small (i.e. non-saline) for all samples ranging from 1.33 mS m^{-1} to 42.6 mS m^{-1} for the topsoils and 1.24 mS m^{-1} to 13.7 mS m^{-1} for the subsoils. Cation exchange capacity (CEC) of soils was mostly small, ranging between 69.8 $mmol_c$ kg^{-1} and 99.7 $mmol_c$ kg^{-1} for the topsoils and between 47.4 $mmol_c$ kg^{-1} and 99.7 $mmol_c$ kg^{-1} for the subsoils. The clay content in soils increased with depth and it ranged from 3 to 54 % in the topsoils and 6 to 59 % in the subsoils. Total Al increased significantly with depth, while total Fe, Mn and Si concentration remained similar.

The concentrations of TC and TN were significantly ($p<0.05$) greater in the topsoils (TC: 25.0±2.3 g kg^{-1} and TN: 1.2±0.2 g kg^{-1}) than the subsoils (TC: 17.5±1.6 and TN: 0.7±0.1 g kg^{-1}) as shown in Fig. S1. A linear relationship was observed between TC and TN in the topsoils (R^2 = 0.60, $p<0.001$), subsoils (R^2 = 0.78, $p<0.001$), and all samples combined (topsoils and subsoils) (R^2 = 0.75, $p<0.001$) (Fig. S2). The C:N ratio significantly ($p<0.05$) increased with soil depth, from 23.3±1.3 in the topsoils to 28.7±1.8 in the subsoils.

The correlation coefficients between soil physical and chemical properties are shown in Table 3. The CEC showed a significant positive correlation with the clay content (r = 0.70, $p<0.01$) and a significant negative correlation with sand content (r = - 0.64, $p<0.01$). Soil pH showed significant positive correlations with CEC, exchangeable Ca, exchangeable Mg, exchangeable Na, and clay content. Soil EC had significant positive relationships with TC, TN, exchangeable Ca, exchangeable K, and CEC.

Total Fe and Al showed significant positive correlations with clay and CEC. Total Mn had significant positive relationships with pH, EC, TC, TN, exchangeable Ca, exchangeable K, CEC, and total Fe. Total Si showed a significant positive relationship with sand content (r = 0.71, $p<0.01$).

https://doi.org/10.5194/egusphere-2026-2843
Preprint. Discussion started: 25 August 2026

Table 2. Summary of important chemical and physical properties of the studied soils (n = 74)

Properties	Topsoil			Subsoil		
	Range	Mean ± SE	Median	Range	Mean	Median
pH $_{(1:5\ water)}$	4.70 – 7.38	5.92±0.11a	5.85	4.87 – 7.60	6.15±0.13a	6.14
$EC_{1:5}$ (mS m^{-1})	1.33 – 42.6	6.73±1.13a	4.99	1.24 – 13.7	4.18±0.44b	3.43
CEC ($mmol_c\ kg^{-1}$)	69.8 – 99.7	94.0±1.3a	97.9	47.4 – 99.7	92.5±2.1a	98.3
Exchangeable Ca ($mmol_c\ kg^{-1}$)	1.3 – 37.9	18.0±1.9a	20.9	0.6 – 39.8	15.7±1.9a	13.4
Exchangeable Mg ($mmol_c\ kg^{-1}$)	2.3 – 34.7	16.0±1.4a	16.4	1.8 – 49.9	18.3±1.8a	15.4
Exchangeable Na ($mmol_c\ kg^{-1}$)	0.1 – 13.4	1.5±0.4a	1	0.1 – 23	3.8±0.9b	1.3
Exchangeable K ($mmol_c\ kg^{-1}$)	0.4 – 7.6	2.5±0.3a	2.2	0.1 – 6.1	1.5±0.2b	1.1
Sand (%)	36 – 95	61.7±2.9a	64	26 – 90	56.9±2.9a	59
Silt (%)	2 – 30	13.2±1.0a	14	2 – 30	11.9±1.1a	11
Clay (%)	3 – 54	25.1±2.6a	20	6 – 59	31.2±2.7a	30
Total Fe ($g\ kg^{-1}$)	9.34 – 161.97	50.12±5.91a	35.12	11.26– 136.96	53.29±5.17a	40.83
Total Al ($g\ kg^{-1}$)	18.08– 125.79	76.54±3.99a	77.72	40.18– 132.91	87.31±3.34b	88.16
Total Mn ($g\ kg^{-1}$)	0 – 3.1	0.78±0.13a	0.5	0 – 3.6	0.60±0.13a	0.3
Total Si ($g\ kg^{-1}$)	148.54– 384.73	251.42±9.35a	258.32	153.39– 356.31	237.33±8.26a	235.71

Similar letters in the same row indicate non-significant differences between mean values ($P < 0.05$) while different letters indicate significant differences between mean values ($P < 0.05$) of soil properties.

Table 3: Spearman's rho correlation coefficients for relationships between soil physical and chemical properties.

	pH	EC	TC	TN	Ca	Mg	Na	K
EC	0.25*							
TC	-0.06	0.40**						
TN	<0.1	0.58**	0.84**					
Ca	0.58**	0.51**	0.18	0.39**				
Mg	0.38**	0.13	-0.04	-0.01	0.14			
Na	0.24*	-0.03	-0.06	-0.11	-0.08	0.56**		
K	0.05	0.61**	0.36**	0.54**	0.47**	-0.02	-0.13	
CEC	0.57**	0.23*	0.02	0.11	0.51**	0.73**	0.44**	0.04
Sand	-0.22	0.05	0.01	-0.05	-0.22	-0.55**	-0.27*	0.22
Silt	<-0.1	0.22	0.24*	0.29*	0.20	0.13	0.14	0.23*
Clay	0.27*	-0.08	-0.06	<-0.1	0.25*	0.60**	0.30**	-0.24*
Total Fe	0.32**	-0.03	0.07	0.12	0.29*	0.56**	0.18	-0.28*
Total Al	0.14	-0.31**	-0.06	-0.14	-0.04	0.47**	0.19	-0.40**
Total Mn	0.49**	0.33**	0.27*	0.53**	0.66**	0..08	-0.16	0.34**
Total Si	-0.25*	0.07	-0.14	-0.11	-0.22	-0.48**	-0.14	0.30**

**Correlation significant at $P < 0.01$.
*Correlation significant at $P < 0.05$.

https://doi.org/10.5194/egusphere-2026-2843
Preprint. Discussion started: 25 August 2026

Table 3 continued:

	CEC	Sand	Silt	Clay	Total Fe	Total Al	Total Mn
Sand	-0.64**						
Silt	0.22	-0.50**					
Clay	0.70**	-0.94**	0.22				
Total Fe	0.69**	-0.76**	0.16	0.81**			
Total Al	0.42**	-0.73**	0.03	0.81**	0.75**		
Total Mn	0.30**	-0.12	0.23	0.08	0.25*	-0.13	
Total Si	-0.60**	0.71**	-0.07	-0.78**	-0.89**	-0.84**	-0.14

**Correlation significant at P < 0.01.
*Correlation significant at P < 0.05.

3.2. Extractable Fe, Al, Mn and Si concentrations

The concentration of Fe extracted for the three extractants was in the sequence – Fe_{DCB} > Fe_{OX} > Fe_{PP} (Fig. 2a). The Fe_{PP} concentration in all soil samples ranged from 0.01 g kg^{-1} to 5.80 g kg^{-1}, with a significantly ($p<0.001$) greater mean concentration in the topsoils (1.10±0.11 g kg^{-1}) than the subsoils (0.85±0.12 g kg^{-1}). The Fe_{OX} concentration varied between 0.68 g kg^{-1} and 12.81 g kg^{-1}, and the topsoils (4.15±0.33 g kg^{-1}) and subsoils (3.99±0.33 g kg^{-1} having a similar mean concentration. Fe_{DCB} concentration in soil samples ranged from 2.92 g kg^{-1} to 79.87 g kg^{-1}, and like Fe_{OX}, the mean Fe_{DCB} concentration was similar in the topsoils (23.46±1.87 g kg^{-1}) and the subsoils (25.76±1.94 g kg^{-1}) (Fig. 2a). On an average, PP, OX and DCB extracted 3±0.03 %, 9±0.05 % and 49±0.18 % of the total Fe, respectively, across both soil depths.

The concentration of Al dissolved by the three extractants was in the order: Al_{DCB} > Al_{OX} > Al_{PP} (Fig. 2b). The Al_{PP} concentration ranged between 0.27 g kg^{-1} and 6.47 g kg^{-1}, with similar average concentrations in the topsoils (1.41±0.11 g kg^{-1}) and the subsoils (1.39±0.13 g kg^{-1}). Al_{OX} concentration varied from 0.34 g kg^{-1} to 8.0 g kg^{-1}, with a significantly ($p=0.003$) greater concentration in the subsoils (3.31±0.21 g kg^{-1}) than the topsoils (3.00±0.20 g kg^{-1}). The Al_{DCB} concentration in soils ranged from 0.28 g kg^{-1} to 10.26 g kg^{-1}, with a mean of 2.94±0.2 g kg^{-1} in the topsoils and 3.50±0.25 g kg^{-1} in the subsoils. The subsoils had a significantly ($p=0.008$) greater mean concentration of Al_{DCB} than the topsoils. PP, OX and DCB extracted Al constituted on an average 2±0.01 %, 3.9±0.02 %, and 4±0.02 %, respectively, of the total Al in all samples.

Unlike Fe and Al, more Mn was extracted by OX than DCB, with the order being – Mn_{OX} > Mn_{DCB} > Mn_{PP} (Fig. 2c). The concentration of Mn in all three extractions was generally very low, with values < 1.1 g kg^{-1} in all samples. The Mn_{PP} concentration ranged from <0.01 g kg^{-1} to 1.07 g kg^{-1} and the topsoils (0.25±0.03 g kg^{-1}) having a significantly ($p<0.001$) greater concentration than the subsoils (0.11±0.01 g kg^{-1}). The concentrations of Mn_{OX} in soil samples varied from 0.001 to 2.93 g kg^{-1} and it was also significantly ($p<0.001$) greater in the topsoils (mean = 0.60±0.08 g kg^{-1}) than the mean concentration in the subsoils (0.45±0.08 g kg^{-1}). DCB extracted Mn concentration ranged from 0.01 g kg^{-1} to 3.62 g kg^{-1}, and like Mn_{PP} and Mn_{OX}, the topsoils (0.47±0.07 g kg^{-1}) had a significantly ($p=0.04$) greater mean concentration of Mn_{DCB} than the subsoils (0.36±0.07 g kg^{-1}). PP, OX and DCB extracted on an average 43±1.23 %, 78±1.58 % and 65±1.10 % of the total Mn, respectively, across both soil depths.

The concentration of Si dissolved by the three extractants occurred in the sequence – Si_{DCB} > Si_{OX} > Si_{PP} (Fig. 2d). The concentration of Si_{PP} ranged from 0.19 g kg^{-1} to 2.45 g kg^{-1}, with similar concentrations in the topsoils (0.69±0.03 g kg^{-1}) and subsoils (0.66±0.05 g kg^{-1}). Si_{OX}

https://doi.org/10.5194/egusphere-2026-2843
Preprint. Discussion started: 25 August 2026

concentrations varied between 0.05 g kg^{-1} and 3.03 g kg^{-1}, with significantly (p=0.006) greater concentration in the subsoils (0.81±0.07 g kg^{-1}) than the topsoils (0.70±0.06 g kg^{-1}). The concentration of Si_{DCB} ranged from 0.28 g kg^{-1} to 4.35 g kg^{-1}, and the subsoils (1.76±0.11 g kg^{-1}) had a significantly (p=0.07) greater mean concentration of Si_{DCB} than the topsoils (1.52±0.08 g kg^{-1}). PP extracted 0.3±0.001 % (mean) of the total Si, OX extracted 0.4±0.003 % of the total Si, and DCB extracted 0.7±0.01 % of the total Si across both depths.

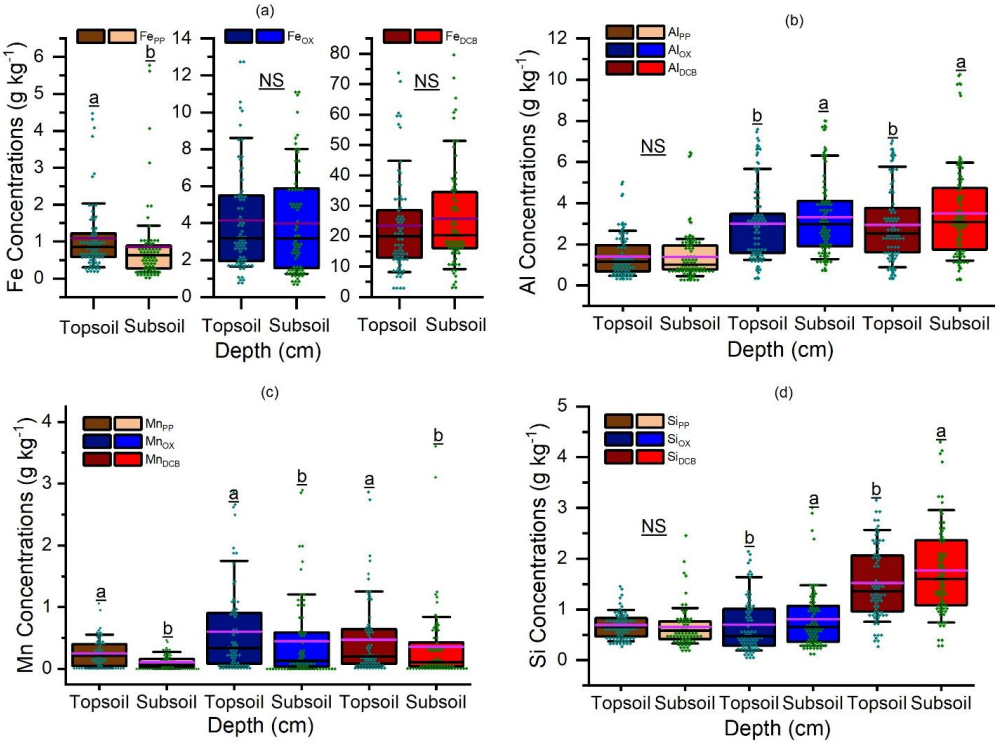

Figure 2. Concentrations of iron (Fe), aluminium (Al), manganese (Mn) and silicon (Si) in topsoils and subsoils extracted by sodium pyrophosphate (PP), ammonium oxalate (OX), and dithionite-citrate-bicarbonate (DCB) procedures. Boxes comprise of the 25th and 75th percentiles, whiskers extend from the 10th to 90th percentiles. Purple and black bars signify the mean and the median values, respectively. Dark cyan and green diamonds indicate data for individual samples; the symbols are displaced horizontally to avoid overlaps. Different letters indicate significant differences in the mean values between samples from different soil depths based on paired T-test (p<0.05). NS means non-significant difference.

https://doi.org/10.5194/egusphere-2026-2843
Preprint. Discussion started: 25 August 2026

3.3. Relationship between extractable metal(loid)s

The Pearson correlation coefficients between extractable metals are shown in Table 4. Fe_{OX} showed a significant positive correlation with all other extractable forms of Fe, Al, Si, and Mn. Fe_{DCB} was positively and significantly correlated with Al_{OX}, Al_{DCB}, Mn_{OX}, Mn_{DCB}, Mn_{PP}, Si_{OX}, Si_{DCB}, and negatively and significantly correlated with Si_{PP}. Fe_{PP} showed significant positive correlations with Al_{OX} and Al_{PP}.

Al_{OX} had significant positive relationships with Al_{DCB}, Al_{PP}, and Si_{OX}. Al_{DCB} showed significant positive relationships with Al_{PP}, Si_{OX}, Si_{DCB} and a significant negative relationship with Si_{PP}. Al_{PP} showed a significant negative correlation with Mn_{OX}, Mn_{DCB}, and Si_{DCB}. Mn_{OX} had a significant positive correlation with Mn_{DCB}, Mn_{PP}, Si_{OX}, and Si_{DCB}, while Mn_{DCB} had a significant positive correlation with Mn_{PP}. Si_{OX} and Si_{PP} showed a significant positive relationship with Si_{DCB}.

Table 4: Pearson correlation coefficients for relationships between different extractable metal(loid)s in soils

	Fe_{OX}	Fe_{DCB}	Fe_{PP}	Al_{OX}	Al_{DCB}	Al_{PP}	Mn_{OX}	Mn_{DCB}	Mn_{PP}	Si_{OX}	Si_{DCB}
Fe_{DCB}	0.61**										
Fe_{PP}	0.41**	0.04									
Al_{OX}	0.64**	0.50**	0.24*								
Al_{DCB}	0.48**	0.83**	0.16	0.69**							
Al_{PP}	0.26*	0.06	0.64**	0.65**	0.40**						
Mn_{OX}	0.46**	0.39**	0.01	-0.07	0.05	-0.30**					
Mn_{DCB}	0.42**	0.34**	0.06	-0.10	0.05	-0.27*	0.93**				
Mn_{PP}	0.36**	0.29*	0.22	-0.17	-0.05	-0.23	0.77*	0.63**			
Si_{OX}	0.71**	0.44**	-0.10	0.51**	0.30**	-0.11	0.29*	0.19	0.09		
Si_{DCB}	0.35**	0.45**	-0.21	0.20	0.26*	-0.23*	0.25*	0.21	0.05	0.55**	
Si_{PP}	<0.01	-0.24*	0.12	-0.17	-0.37**	-0.03	0.10	0.02	0.16	0.13	0.32**

** Correlation significant at the 0.01 probability level (2-tailed).

* Correlation significant at the 0.05 probability level (2-tailed).

3.4. Extractable C concentrations

Organic C was dissolved by the three extractants in the sequence – $C_{PP} > C_{DCB} > C_{OX}$ (Fig. 3). The PP extracted C (C_{PP}) ranged from 2.8 to 31.0 g kg^{-1} with a mean of 13.3±1.17 g kg^{-1} in the topsoils and 11.9±1.14 g kg^{-1} in the subsoils. The mean C_{PP} concentration was significantly greater (p=0.004) in the topsoils than the subsoils. Sodium pyrophosphate extracted on an average 62±0.2 % of the total soil C across both soil depths.

The concentration of DCB extractable C (C_{DCB}) ranged from 0.5 g kg^{-1} to 28.4 g kg^{-1} in all samples, with a significantly (p=0.025) greater mean concentration in the topsoils (9.8±1.25 g kg^{-1}) than in the subsoils (8.5±1.11 g kg^{-1}) (Fig. 3). The extractable C_{DCB} constituted 41±0.2 % (mean) of the total soil C across both depths.

The OX extractable C (C_{OX}) concentration varied between 0.5 g kg^{-1} and 26.5 g kg^{-1} across the two depths. The concentration was similar in the topsoils (6.4±1.08 g kg^{-1}) and subsoils (6.3±1.11 g kg^{-1}) (Fig. 3). The C_{OX} represented on an average 28±0.2 % of the total C in all samples.

The concentration of the DCB extractable C minus OX extractable C ($C_{DCB} – C_{OX}$), i.e., C associated only with crystalline forms of Fe oxides was similar in the topsoils (3.3±0.55 g kg^{-1}) and the subsoils (2.29±0.28 g kg^{-1}) (Fig. 3). The $C_{DCB} – C_{OX}$ constituted on the average 13±0.2 % of the total soil C across both depths.

https://doi.org/10.5194/egusphere-2026-2843
Preprint. Discussion started: 25 August 2026

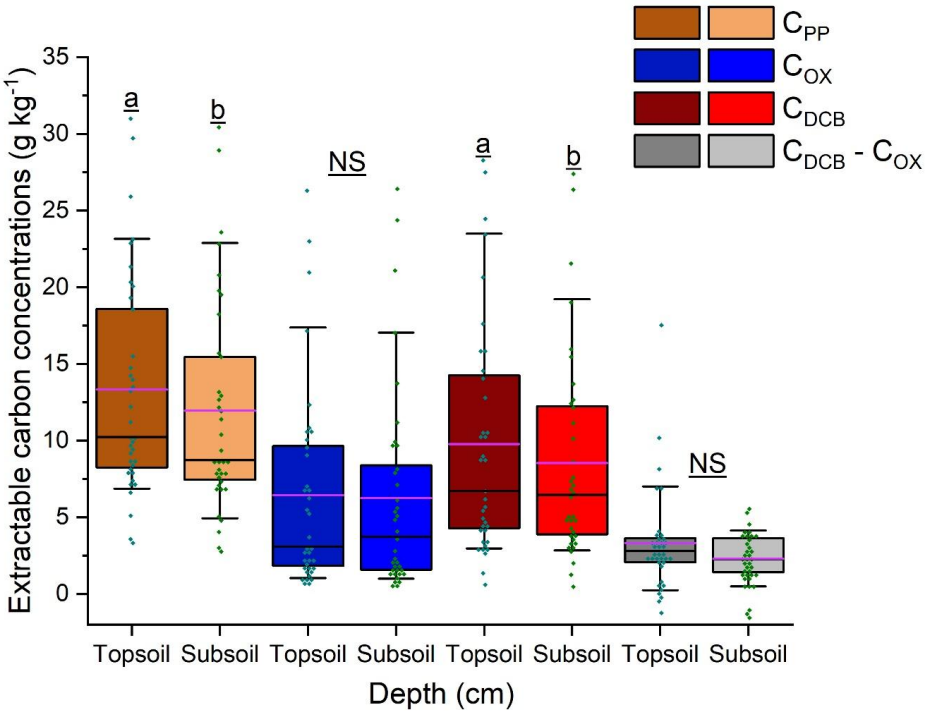

Figure 3. Concentrations of carbon (C) in topsoils and subsoils extracted by sodium pyrophosphate (PP), ammonium oxalate (OX), dithionite-citrate-bicarbonate (DCB) reagents, and concentration of carbon extracted by dithionite-citrate-bicarbonate (DCB) minus concentration of carbon extracted by ammonium oxalate (OX). Boxes comprise of the 25th and 75th percentiles, whiskers extend from the 10th to 90th percentiles. Purple and black bars signify the mean and the median values, respectively. Dark cyan and green diamonds indicate data for individual samples; the symbols are displaced horizontally to avoid overlaps. Different letters indicate significant differences in the mean values of samples from different soil depths based on paired T-test ($p<0.05$). NS means non-significant difference.

3.5. Relationship between extractable metal phases, soil properties and extractable C

Relationships between extractable metals, extractable C and soil properties using the generalized linear mixed model (GLMM) regression are shown in Tables 5 and 6. When TC was included as a fixed effect term into the model (Table 5), different forms of extractable metals showed no significant relationship with the extractable forms of C in both top- and sub-soils except for significant negative relationships of Fe_{OX} (topsoil), Al_{OX} and Al_{DCB} (subsoil) with extractable C. However, the TC showed significant ($p<0.001$) relationships with the different extractable forms of C in both topsoils and subsoils (Table 5). In addition, pH had a significant relationship with the three forms of extractable C in the topsoils. Clay content also showed a significant relationship with all three forms of extractable C in the subsoils, whereas silt showed a significant relationship with C_{OX} ($p<0.001$) and C_{DCB}, ($p=0.01$) in the topsoils.

When TC was excluded from the generalized linear mixed model (GLMM), the three forms of extractable C showed positive relationships with pH, silt or clay and extractable Fe and Al

https://doi.org/10.5194/egusphere-2026-2843
Preprint. Discussion started: 25 August 2026

(Table 6). For example, Fe_{PP}, pH, and silt showed statistically significant ($p<0.001$, $p<0.001$, and $p=0.0004$, respectively) relationships with C_{PP} in the topsoils. Fe_{OX} and pH had significant positive ($p<0.001$ and $p=0.026$, respectively) relationships with C_{OX} in the topsoils, and Fe_{OX}, pH, and silt ($p<0.001$) had significant positive relationships with C_{OX} in the subsoils. Also, Al_{DCB} ($p<0.001$) and pH ($p=0.002$) showed significant positive relationships with C_{DCB} in the topsoils; and Fe_{DCB} ($p<0.001$) and silt ($p=0.0006$) showed significant positive relationships with C_{DCB} in the subsoils.

3.6. Extractable C: metal molar ratio

The molar ratio of C to metals (C: M (or Fe+Al)) extracted by each reagent in the samples from two depths are presented in Fig. 4. In the PP extracts, the C:M molar ratio for all samples varied between 1.2 and 40.9 and it was similar for the topsoils (9.4±1.3) and subsoils (9.6±1.4) (Fig. 4a). The C:M molar ratio in the OX extracts ranged from 0.1 to 10.7, with a similar mean value of 1.6±0.3 and 1.4±0.3 for the topsoils and the subsoils (Fig. 4b), respectively. The C:M molar ratio in the DCB extracts ranged from 0.03 to 8.5 in all samples and also had similar mean ratios in the topsoils (1.0±0.2) and subsoils (0.7±0.1) (Fig. 4c).

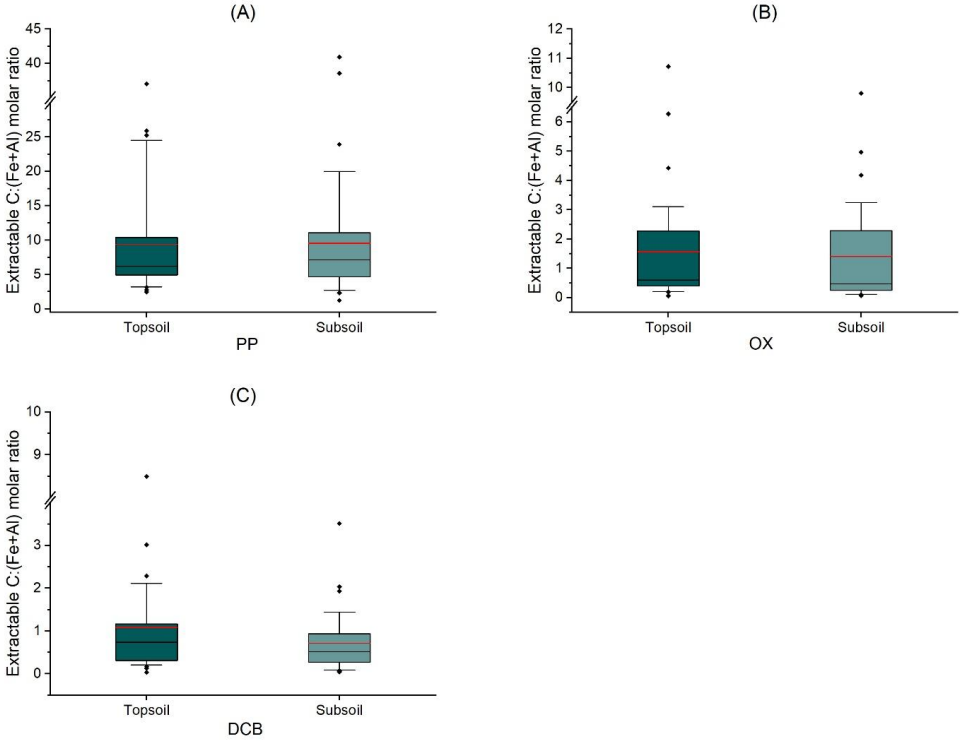

Figure 4. Boxplots of C:(Fe+Al) molar ratios in the extracts of sodium pyrophosphate (PP), ammonium oxalate (OX), and dithionite-citrate-bicarbonate (DCB) of topsoils and subsoils. Boxes comprise of the 25th and 75th percentiles, whiskers extend from the 10th to 90th percentiles, red bars signify mean, black bars signify median, and black dots show the outliers.

https://doi.org/10.5194/egusphere-2026-2843
Preprint. Discussion started: 25 August 2026

Table 5. Fixed effect parameter estimates in the topsoils and subsoils obtained from the generalized linear mixed model. The extractable metals and soil properties (including TC) were used as the fixed effect terms, soil types as the random effect and sodium pyrophosphate extractable C, ammonium oxalate extractable C and dithionite-citrate-bicarbonate extractable C as the dependent variables. The standard errors are given in parentheses.

	Depth	Fixed effect term	Regression coefficient	95 % Lower	95% Upper	F Ratio	Prob>F
C_{PP}	Topsoil	Fe_{PP}	0.06 (0.06)	-0.06	0.19	1.06	0.31
		pH	0.26 (0.08)	0.08	0.43	9.51	0.005
		TC	0.02 (0.003)	0.01	0.03	31.58	<0.001
		Intercept	0.002 (0.01)	-0.02	0.02		
	Subsoil	Fe_{PP}	0.05 (0.09)	-0.24	0.14	0.31	0.58
		Al_{PP}	0.08 (0.07)	-0.22	0.17	1.22	0.28
		Clay	0.01 (0.004)	8.08	0.003	0.02	0.007
		TC	0.05 (0.01)	0.04	0.07	48.57	<0.001
		Intercept	-0.001 (0.01)	-0.02	0.02		
C_{OX}	Topsoil	Fe_{OX}	-0.09 (0.04)	-0.16	-0.01	5.99	0.02
		pH	0.56 (0.130	19.84	0.26	0.87	0.004
		Silt	0.06 (0.01)	0.04	0.09	25.80	<0.001
		TC	0.04 (0.01)	0.02	0.05	38.18	<0.001
		Intercept	0.004 (0.03)	-0.05	0.06		
	Subsoil	Fe_{OX}	-0.11 (0.04)	-0.19	-0.02	7.21	0.011
		Al_{OX}	-0.15 (0.06)	-0.26	-0.03	6.32	0.017
		Clay	0.02 (0.01)	0.01	0.03	8.40	0.007
		TC	0.09 (0.01)	0.07	0.11	86.31	<0.001
		Intercept	0.05 (0.06)	-0.07	0.16		
C_{DCB}	Topsoil	Fe_{DCB}	0.02 (0.01)	-0.01	0.02	0.52	0.47
		Al_{DCB}	-0.10 (0.09)	-0.29	0.09	1.13	0.30
		pH	0.26 (0.12)	0.01	0.52	4.78	0.04
		EC	-0.06 (0.01)	-0.08	-0.04	29.11	<0.001
		Silt	0.03 (0.01)	0.01	0.05	7.79	0.01
		TC	0.06 (0.01)	0.05	0.07	92.56	<0.001
		Intercept	0.01 (0.02)	-0.03	0.05		
	Subsoil	Fe_{DCB}	-0.001 (0.01)	-0.01	0.01	0.05	0.83
		Al_{DCB}	-0.10 (0.05)	-0.21	0.01	3.50	0.07
		Clay	0.01 (0.01)	0.001	0.02	5.26	0.03
		TC	0.06 (0.01)	0.05	0.07	77.69	<0.001
		Intercept	0.05 (0.05)	-0.05	0.15		

https://doi.org/10.5194/egusphere-2026-2843
Preprint. Discussion started: 25 August 2026

Table 6. Fixed effect parameter estimates in the topsoils and subsoils obtained from the generalized linear mixed model. The extractable metals and soil properties (excluding the TC) were used as the fixed effect terms, soil types as the random effect and sodium pyrophosphate extractable C, ammonium oxalate extractable C and dithionite-citrate-bicarbonate extractable C as the dependent variables. The standard errors are given in parentheses.

	Depth	Fixed effect term	Regression coefficient	95 % Lower	95% Upper	F Ratio	Prob>F
C_{PP}	Topsoil	Fe_{PP}	0.23 (0.03)	0.17	0.30	53.96	<0.001
		pH	0.27 (0.06)	0.16	0.38	22.56	<0.001
		Silt	0.02 (0.01)	0.01	0.03	14.12	0.0004
		Intercept	0.37 (0.37)	-0.37	1.11		
	Subsoil	Fe_{PP}	0.30 (0.04)	0.21	0.38	44.45	<0.001
		Al_{PP}	0.14 (0.05)	0.23	0.44	8.67	0.004
		Clay	0.01 (0.003)	0.002	0.01	7.34	0.009
		Intercept	2.17 (0.11)	1.92	2.41		
C_{OX}	Topsoil	Fe_{OX}	0.08 (0.02)	0.04	0.12	18.03	<0.001
		pH	0.18 (0.08)	0.02	0.34	5.16	0.026
		Intercept	0.30 (0.51)	-0.72	1.33		
	Subsoil	Fe_{OX}	0.14 (0.02)	0.09	0.18	33.09	<0.001
		Si_{OX}	-0.52 (0.19)	-0.77	-0.27	17.76	<0.001
		pH	0.35 (0.08)	0.19	0.52	18.44	<0.001
		Silt	0.04 (0.01)	0.02	0.06	29.84	<0.001
		Intercept	-1.15 (0.53)	-2.22	-0.09		
C_{DCB}	Topsoil	Al_{DCB}	0.22 (0.04)	0.15	0.29	36.47	<0.001
		pH	0.24 (0.07)	0.09	0.39	10.22	0.002
		EC	0.03 (0.01)	0.01	0.04	20.98	<0.001
		Clay	-0.01 (0.003)	-0.02	-0.002	5.92	0.018
		Intercept	-0.16 (0.58)	-1.33	1.02		
	Subsoil	Fe_{DCB}	0.02 (0.003)	0.01	0.02	23.48	<0.001
		Silt	0.02 (0.01)	0.01	0.04	13.08	0.0006
		Intercept	1.33 (0.24)	0.78	1.87		

https://doi.org/10.5194/egusphere-2026-2843
Preprint. Discussion started: 25 August 2026

4 Discussion

4.1 Soil physicochemical properties in relation to OC

The association of OC with Fe and Al oxides can be affected by soil pH, which influences mineral phases of Fe and Al oxides, surface charge characteristics of these oxides, and chemical interactions between OC and metal oxides (Zhao et al., 2016; Ye et al., 2022). Most of the soils had acidic pH and a significant positive relationship was observed between soil pH and extractable C (Tables 5 and 6). Both Fe and Al oxides carry a net positive charge in the acidic to near neutral pH range, as the point of zero charge of these minerals range from 7.8 to 10 (Sparks et al., 2024). Also, a net negative charge on soil organic matter would be expected under these pH conditions, which increases with increasing pH due to deprotonation of acidic functional groups of OC, such as carboxyls, quinones and enols (Sparks et al., 2024). Other studies have observed a significant correlation between soil pH and Fe/Al associated OC, which implies that soil pH regulates the propensity of Fe and Al oxides to associate with OC (Wang et al., 2017; Zhao et al., 2019; Ye et al., 2022).

The significant positive relationships between extractable C, clay and silt (Table 5 and 6) indicates the important role of the fine soil fractions in stabilising OC in soils, which is consistent with several previous studies (Six et al., 2002; Jindaluang et al., 2013; Yu et al., 2019). Soil clay fraction is important in stabilising OC, with its ability to protect OC via physical and chemical interactions and other indirect factors. Oades (1988) suggested that finer textured soils have more cation bridges (Ca^{2+} in neutral, Fe^{3+} and Al^{3+} in acidic soils) to bind organic molecules to negatively charged soil clay particles. While Christensen (1992) supported the idea of increased binding of organic molecules via cation bridges in clayey soils, he proposed that the principal effect of higher clay (or clay + silt) contents occurred via stabilisation of microbially processed of organic residues, that are readily lost in sandy soils. In contrast, Feller et al. (2020) concluded that greater biomass inputs or aggregation in finer textured soils caused correlations between SOC and clay concentrations in tropical soils. It has been reported that there is a greater amount of MAOM in soils with increased clay and silt contents, and hence increased OM storage through binding to mineral surfaces in soils (Stewart et al., 2007; Laganière et al., 2010; Vos et al., 2018). Others have suggested increased occlusion of particulate OM in soil aggregates rich in clay-size minerals that restricts access for microbial degradation (McCarthy et al., 2008; Steffens et al., 2017; Schweizer et al., 2021). Jindaluang et al. (2013) reported that organic compounds with aromatic and amide functional groups are selectively preserved in fine textured soils, while recalcitrant aliphatic-C existed in the coarse textured soils. Hassink (1997) proposed that C associated with organo-mineral complexes are protected chemically and the level of protection increased with increased silt fraction in the soil. It is possible that all or many of these mechanisms occur simultaneously, but the adsorption of organic compounds to clay surfaces appeared to be a major factor in the preservation of SOM.

4.2 Extractable metal(loid)s

The dissolution of metal(loid)s during PP, OX and DCB extractions provides an approximation of their specific phases in soils, acknowledging that these extractions are not completely selective and often some overlaps exist in the extracted fractions of metal(loid)s (Parfitt, 2009; Rennert, 2019). In addition, re-adsorption of some extracted OC can also occur in the

https://doi.org/10.5194/egusphere-2026-2843
Preprint. Discussion started: 25 August 2026

extraction procedure. Nevertheless, chemical extraction procedures offer the best option for routine evaluation of OC association with different chemical and mineralogical phases of metal(loid)s in large number of soil samples. The extracted concentration of Fe, Al, and Si followed the same sequence (i.e., DCB > OX >PP), while Mn was extracted in the sequence – OX > DCB > PP.

The DCB procedure is known to extract pedogenic or free Fe oxides (and Al substituted in the structure of goethite and hematite) as well as poorly crystalline and SRO Fe/Al oxides (Mckeague and Day, 1966; Shang and Zelazny, 2008). The large proportion of the total Fe extracted by the DCB procedure reflected high concentration of secondary Fe oxides in the studied soils. This partly support our hypothesis that concentration of extractable Fe will be the most prominent element in the soils. In addition to the targeted phases, the DCB procedure may also extract a fraction of organic complexed Fe from soils (Bascomb, 1968), while some Fe oxides (such as magnetite and maghemite) and Fe sulfides are only partially or not extracted in the DCB extraction procedure (Pansu and Gautheyrou, 2006; Rennert and Lenhardt, 2025). In the oxalate extraction procedure, Fe present in non-crystalline, poorly ordered and short-range ordered (such as ferrihydrite) was dissolved and a fraction in the organic complexes may also be dissolved (Schwertmann, 1964; Mckeague and Day, 1966; Bascomb, 1968; Loeppert and Inskeep, 1996; Mikutta et al., 2006). Oxalate extracted Fe had often been used to estimate ferrihydrite, a short range ordered Fe oxide phase, concentrations in soils (Carlson and Schwertmann, 1981; Schwertmann et al., 1982). The small ratio of Fe_{OX}:Fe_{DCB}, referred to as active Fe ratio, indicate the degree of crystallinity of Fe oxides in soils (Mckeague and Day, 1966). In topsoils and subsoils, the mean value of Fe_{OX}:Fe_{DCB} ratio was 0.18 and 0.16 (< 0.2), respectively, which suggest that most of the Fe was present in crystalline Fe oxides (i.e., goethite and hematite) in soils and the content of poorly crystalline Fe phases was small irrespective of soil depth (Mikutta et al., 2006). The significant correlation between Fe_{DCB} and Fe_{OX} (Table 4), may be due to some overlap in the phases extracted by the two procedures. The DCB method is known to extract both crystalline and SRO (and poorly crystalline) Fe oxides from soils (Mckeague and Day, 1966; Shang and Zelazny, 2008). In addition to SRO Fe oxides, oxalate is known to dissolve crystalline Fe oxides, such as magnetite, maghemite, lepidocrocite, and poorly crystalline and nano-crystalline goethite and hematite (Childs and Wilson, 1983; Walker, 1983; Mansfeldt et al., 2012). The close relationship between Fe_{DCB} and Fe_{OX} may also suggest that both Fe forms were function of similar pedogenic processes (Rezapour et al., 2015).

Pyrophosphate (at pH 10) has been considered as a good extractant for organic Fe and Al complexes and 'active' amorphous inorganic forms of Fe from soils (Bascomb, 1968; Loveland and Digby, 1984; Pansu and Gautheyrou, 2006). Fe_{PP} concentration in soils was generally small and decreased with soil depth (Fig. 2a), a trend similar to the OC concentration in soils (Fig. S1). These results are consistent with the published data for non-podzolic soils (Bascomb, 1968; Daly, 1982; Parfitt and Childs, 1988). Large variations in the Fe_{PP} concentration with different centrifugation speeds and/or use of flocculating agents have been observed in several past studies (Jeanroy and Guillet, 1981; McKeague and Schuppli, 1982; Schuppli et al., 1983; Loveland and Digby, 1984; Skjemstad et al., 1990). The variability in the Fe_{PP} concentration had also been attributed to peptization of micro-crystalline goethite (including Al-substituted goethite) and ferrihydrite on which organic matter had been adsorbed (Borggaard, 1988; Parfitt and Childs, 1988; Rennert, 2019). There was no clear evidence for the presence of any solid phase in the supernatant in the procedure with medium-speed centrifugation (3280 × *g*) followed by micro-filtration (0.2 µm). On the contrary, Ruiz et al.

https://doi.org/10.5194/egusphere-2026-2843
Preprint. Discussion started: 25 August 2026

(2026) reported visual evident for the presence of suspended fine particles during filtration procedure, indicating colloidal dispersion. Most of the soils used in this study had acidic pH and moderate amount of Al. The presence of Al, and the use of medium-speed centrifugation and micro-filtration may have mitigated the dispersion of colloidal materials in these soils. The Fe_{PP} concentration data were consistent with the results obtained in other studies that used high-speed centrifugation and/or ultrafiltration (Schuppli et al., 1983; Loveland and Digby, 1984). The significant correlation between Fe_{PP} and Fe_{OX} (Table 4) suggests some overlapping extractions of amorphous and SRO phases and Fe-organic complexes by the two reagents (Bascomb, 1968; Higashi et al., 1981; Jeanroy and Guillet, 1981).

The differences between the mean Al_{PP}, Al_{OX} and Al_{DCB} concentrations are much smaller compared with the mean Fe concentrations extracted by the three extractants (Fig. 2a and b) and similar results have been obtained in previous studies (Skjemstad et al., 1990; Singh and Gilkes, 1991; Wiriyakitnateekul et al., 2005). Al_{DCB} and Al_{OX} concentrations are similar, with the mean value of Al_{OX}:Al_{DCB} ratio in the topsoils and subsoils being 1.02 and 0.95, respectively. These results are consistent with a large North American soil dataset (Hall and Thompson, 2022). Crystalline Al oxides are generally not dissolved during the DCB extraction and Al in DCB extracts results from various sources, including Al-organic complexes, Al adsorbed on Fe oxides, and Al-substituted in the structure of Fe oxides (Rennert, 2019) . A significant positive correlation was found between Al_{DCB} and Al_{OX} fractions (Table 4), which reflects that the two reagents might have extracted some similar Al-phases, such as, organo-Al complexes (Evans and Smillie, 1976; Parfitt and Childs, 1988; Dahlgren, 1994). The Al_{DCB} concentration showed a very strong correlation with Fe_{DCB} (Table 4), which was possibly due to a concurrent release of Al and Fe from the dissolution of crystalline Fe oxides (i.e., goethite and hematite) during the DCB extraction. Such observations have been made in other studies and Al substitution in goethite (up to 35 mol%) and hematite (up to 23 mol%) is well known in acidic and highly weathered soils (Bigham et al., 1978; Fitzpatrick and Schwertmann, 1982; Childs and Wilson, 1983; Parfitt and Childs, 1988; Singh and Gilkes, 1992). The significant relationship between Al_{PP} and Al_{OX} (Table 4), implies that oxalate may have dissolved Al from organic complexes (Mckeague and Day, 1966; Parfitt and Henmi, 1982; Farmer et al., 1983).

Mn oxides in soils often occur in small concentration and in poorly crystalline forms (Scheinost and Singh, 2023); our results were consistent with this assertion, with Mn mostly being present in poorly crystalline forms that were slightly more efficiently extracted by the oxalate procedure than the DCB procedure. Jarvis (1984) also observed greatest Mn extraction with oxalate from acidic soils, where several extractants including DCB and PP were used. It was speculated that during oxalate extraction Mn was released from the reduction of relatively unweathered, highly crystalline oxides, or from mixed forms of Mn-Fe oxides. Manganese has been found to be strongly associated (adsorbed or substituted in structures) with natural Fe oxides (Singh and Gilkes, 1992). Structural substitution of Mn in synthetic and natural goethite and hematite is well known (Singh and Gilkes, 1992; Manceau et al., 2000; Singh et al., 2000; Singh et al., 2002). The order of Mn concentration extracted by the three extractants in our study is similar to the order obtained for several soils from England (Jarvis, 1984). However, the trend with greater Mn concentrations in the topsoils than the sub soils in our study is opposite to the earlier study, which might be due to the poor drainage and periodic waterlogging conditions in English soils. A significant relationship was observed between Mn_{PP} and Mn_{OX} (Table 4) that is similar to an earlier study; however, the relationship of Mn_{OX} was stronger with Mn_{DCB} than Mn_{PP} (Jarvis, 1984).

https://doi.org/10.5194/egusphere-2026-2843
Preprint. Discussion started: 25 August 2026

Silicon concentrations were small in all three extracts (Fig. 2). These results indicate that poorly crystalline Al-Si phases, such as allophane and imogolite, were absent and there was little or no dissolution of well-crystalline alumino-silicates in the soils (Parfitt and Childs, 1988). The sequence of Si extracted is consistent with the limited published data for the three extractions (Paterson et al., 1993). The highest Si concentration was found in the DCB extracts, which might have released from different sources including adsorbed Si on the surfaces of SRO and crystalline Fe oxides, Si occluded in Fe oxides, and some Si dissolved from micro-crystalline alumino-silicate clay minerals and quartz (Weaver et al., 1968; Gamble and Daniels, 1972; Parfitt and Childs, 1988). Hall and Thompson (2022) reported greater Si in DCB extract than OX extract in soils from all soil orders except Andisols, where the trend was opposite. Fe_{OX} showed a significant correlation with Si_{OX} (Table 4), indicating that Si_{OX} was largely adsorbed onto the surfaces of SRO Fe phases and small amounts may also have been extracted from SRO Fe silicates (Parfitt and Henmi, 1982; Colombo and Torrent, 1991). Non-crystalline Si is not dissolved during the ammonium oxalate extraction (Wada, 1989).

4.3 Organic C association with different fractions of extractable metals

Sodium pyrophosphate is generally assumed to dissolve organo-metal complexes (Bascomb, 1968; Takahashi and Dahlgren, 2016). Pyrophosphate extracted the least amount of Fe, Al, Mn and Si amongst the three extractants (Fig. 2) but dissolved the highest concentration of OC (Fig. 3). Pyrophosphate extractable C constituted an average 62 % (range = 19 - 90 %) of the total SOC content across all samples from both soil depths. Yu et al. (2023) reported 39 to 60 % contribution from C_{PP} to the total SOC, whereas 30 - 43 % contribution to the total SOC was reported in other studies (Wagai et al., 2013; Heckman et al., 2018). A significant positive relationship between Fe_{PP} and C_{PP} in both topsoils and subsoils (Table 6) suggests that organo-Fe complexes were predominantly extracted in the PP procedure. Several other studies have observed significant correlations of Fe_{PP} and Al_{PP} with SOC (Masiello et al., 2004; Wagai et al., 2013; Lawrence et al., 2015; Takahashi and Dahlgren, 2016; Heckman et al., 2018). The association of significant amount of SOC in Fe-organic complexes limits desorption, oxidative degradation, and biodegradation of OC (Parfitt et al., 2002; Kaiser and Guggenberger, 2003; Zimmerman et al., 2004; Rasmussen et al., 2006).

The interpretation of PP extraction data requires some caution due to the dissolution of alkali-induced peptised organic matter (OM) from other fractions (Wagai et al., 2013; Coward et al., 2017). A limited number of samples containing a range of total Fe were extracted with PP at pH 7.5 to evaluate the dissolution of OC due to peptization of Fe/Al oxides adsorbed with organic matter at pH 10 (Parfitt and Childs, 1988; Rennert, 2019). The C_{PP10} and $C_{PP7.5}$ were similar in the four replications of the analysed samples (regression slope = 1.02±0.04, R^2 = 0.97; Fig. S3a). However, the PP at pH 10 extracted nearly three times greater Fe as compared to PP at pH 7.5 (regression slope = 2.88±0.57, R^2 = 0.59; Fig. S3b). The higher Fe extracted at pH 10 than pH 7.5 in this study may be due to the dissolution of Fe from phases other than Fe-organic complexes at higher pH. The other three elements showed variable behaviour, with no consistent trend or relationship between $Al_{PP7.5}$ and Al_{PP10} (Fig. S3c), while Mn_{PP10} and $Mn_{PP7.5}$ concentrations were almost similar (regression slope = 0.85±0.18, R^2 = 0.55; Fig. S3d), and PP at pH 10 extracted about half of the Si concentration as compared to the Si concentration in PP extract at pH 7.5 (regression slope = 0.48±0.09, R^2 = 0.57; Fig. S3e). These results show dissolution of some non-target particles, particularly Fe oxides, at pH 10, however, this did not release any additional OC from the dissolved phases. Ruiz et al. (2026) reported an average of about 46 % greater Fe and Al concentrations extracted with PP at pH

https://doi.org/10.5194/egusphere-2026-2843
Preprint. Discussion started: 25 August 2026

10 than pH 7. PP at pH 10 extracted higher OC concentrations with an average of approximately 40 % compared to PP at pH 7. However, PP can extract poorly and nano crystalline Fe and Al oxides particularly OM complexed by cation bridging. Parfitt and Childs (1988) reported that dispersion typically occurs in clayey soils (> 40 % clay content) containing goethite and ferrihydrite; soils in our study generally had > 40 % clay content, with kaolinite and hydroxy-interlayered vermiculite as the dominant phyllosilicates in the clay fraction.

Short-range-order Fe phases such as ferrihydrite have the capacity to adsorb high concentrations of SOC due to their extensive specific surface area and the presence of reactive sites on surfaces. The significant positive relationship between C_{OX} and Fe_{OX} in the soils (Table 6) suggests that SRO and poorly crystalline Fe oxides contributed substantially to the OC accumulation in the studied soils. About 28 % of the total SOC was solubilised during the OX extraction across both soil depths. Positive correlations between Fe_{OX} and C_{OX} have been reported in several other studies (Kaiser and Guggenberger, 2003; Kleber et al., 2005; Wiseman and Püttmann, 2006; Rasmussen et al., 2018; Yu et al., 2021; Hall and Thompson, 2022; Amenkhienan et al., 2024). Oxalate extractable Si had a significant negative relationship with the C_{OX} in subsoils (Table 6), which suggests that soil samples were devoid of poorly-crystalline aluminosilicates (e.g., allophane and imogolite), which are common in Andosols and Spodosols (Dahlgren, 1994).

Oxalate is a C based complexing agent, hence residual C in soils after OX extraction was compared with C in soils after HH extraction, which does not have C compounds (Heckman et al., 2018). Carbon concentrations extracted by the two reagents in selected samples were quite similar (regression slope between C_{OX} and C_{HH} = 1.18±0.07, R^2 = 0.94; Fig. S4a), which shows that there was little of no C contamination from OX in the OX extraction procedure. In addition, HH and OX extracted similar Fe (regression slope = 1.06±0.07, R^2 = 0.94; Fig. S4b), Al (regression slope = 0.99±0.03, R^2 = 0.98; Fig. S4c) and Mn (regression slope = 0.93±0.02, R^2 = 0.99; Fig. S4d) concentrations, while more Si was dissolved in the HH extraction (regression slope = 0.62±0.05, R^2 = 0.88; Fig. S4e). Hydroxylamine Hydrochloric acid and OX have been reported to have similar ability to extract SRO minerals (Chao and Zhou, 1983), which is consistent with our results.

The C_{DCB} is expected to be C associated with secondary crystalline Fe oxides including SRO phases. In the DCB procedure, 41±0.2 % (mean) of the total SOC was extracted from soil samples from both depths. Since DCB extracts both SRO and crystalline Fe and Al oxides, we calculated the C only in association with well crystalline phases by subtracting the C_{OX} content from the C_{DCB} content for soil samples individually. On an average only 13±0.2 % of the total SOC was found to be associated with crystalline Fe and Al oxides, which shows a relatively small contribution of crystalline Fe oxides in the preservation of OC in the studied soils. The relatively small contribution of crystalline Fe oxides in the preservation of OC might be related to smaller SSA and reduced hydroxyl surface sites of crystalline Fe oxides than to SRO Fe and Al oxides (Mikutta et al., 2006; Heckman et al., 2013; Newcomb et al., 2017; Heckman et al., 2018). Consequently, despite the high concentration of DCB extractable Fe and other elements in the studied soils (Fig. 2a), the C_{DCB} portion was small. In the GLM model, the significant positive relationship between C_{DCB} and Al_{DCB} in topsoils (Table 6), was possibly due to Al substitution in the structure of crystalline Fe oxides (e.g. goethite and hematite) in soils, which dissolved during the DCB extraction. In the subsoils that have small OC concentration, a significant positive relationship existed between C_{DCB} and Fe_{DCB}. In both the top- and sub-soils, Fe_{DCB} showed a similar significant positive relationship with Al_{DCB}, which suggests Al occurred in the structures of goethite and hematite and dissolved during the DCB extraction.

https://doi.org/10.5194/egusphere-2026-2843
Preprint. Discussion started: 25 August 2026

Significant positive correlations between OC and Fe_{DCB}, in soils dominated by crystalline Fe oxides have been observed in past studies (Mikutta et al., 2006; Yeasmin et al., 2017). The C_{DCB} and C_{DH} were similar in the selected samples (regression slope = 1.04±0.05, R^2 = 0.97; Fig. S5a), which showed that no additional C was introduced in soil residues during the DCB extraction. The DH extracted lot less Fe and Al as compared to DCB (Fig. S5b, S5c), which was expected because the DH procedure involved shaking for 16 hours at room temperature, whereas in the DCB method samples were extracted by heating for 15 minutes at 80°C. Mn_{DCB} and Mn_{DH} were similar (Fig. S5d), and the DCB method extracted nearly 1.6 times Si as compared to the DH extraction (Fig. S5e).

4.4 Extractable C: metals (Fe+Al) molar ratio and the potential binding mechanisms

The molar ratio of C:M had been used to describe binding mechanisms between C and Fe + Al metals. The C:M molar ratio provides information on the potential nature and structure of organo-metal associations in the dissolved phases (Kaiser et al., 2007; Huang et al., 2021; Li et al., 2025). Adsorption and co-precipitation experiments have demonstrated that organic functional groups preferentially bind to Fe and Al oxides (Eusterhues et al., 2014; Han et al., 2019; Jardine and Zelazny, 2020; Vance et al., 2020; Li et al., 2023). A C:M molar ratio of 1.0 (C:M = 1.0) indicated the maximum sorption capacity of metals oxides for natural OC (Wagai and Mayer, 2007; Lalonde et al., 2012; Zhao et al., 2016; Coward et al., 2017). Molar ratio values less than 1.0 (C:M < 1.0) suggested the formation of the Fe/Al–associated OC complex via inner-sphere adsorption mechanism (Coward et al., 2018), while C:M values > 1.0, indicated both adsorption and co-precipitation processes co-existed in forming Fe/Al-associated OC complexes. Specifically, C:M values > 6.0, indicated co-precipitation or chelation of organic ligands, generating low-density organic-rich structures forming Fe/Al–associated OC complexes (Higashi, 1983; Guggenberger and Kaiser, 2003; Wagai and Mayer, 2007; Zhao et al., 2016; Coward et al., 2017; Jeewani et al., 2021). Our extraction results suggested the presence of mixed mechanisms for association between C and (Fe+Al) phases in the studied soils. In the PP fractions, high C:M molar ratios indicated the formation of precipitates of Fe/Al-associated OC complexes in both the top- and sub-soils. The PP extraction liberated C from low-density organic dominated structures (Coward et al., 2017; Coward et al., 2018; Jeewani et al., 2021). The OX fractions had C:M molar ratio > 1, suggesting the occurrence of both adsorption and co-precipitation (in organo-metal complexes) processes. In contrast, the relatively low C:M molar ratios in the DCB fraction suggested the adsorption of OC on to crystalline Fe/Al oxides, which possibly occurred via inner-sphere complexation formation (Coward et al., 2017; Jeewani et al., 2021; Yu et al., 2023). The actual mechanisms need to be verified using spectroscopy or other techniques.

5 Conclusions

We determined the association of OC with different fractions of Fe, Al, Mn and Si in top- and sub-soils using chemical extraction procedures. The largest portion (62±0.2 %) of the total OC was found in organo-metal complexes extracted by PP, while about 28±0.2 % of the total OC was associated with SRO phases extracted by OX. Crystalline Fe/Al oxides appeared to play a relatively small role in the stabilisation of OC in the studied soils, with only 13% of the total OC associated with crystalline Fe oxides.

https://doi.org/10.5194/egusphere-2026-2843
Preprint. Discussion started: 25 August 2026

The concentration of extractable Fe was the highest amongst the metal(loid)s in the both top- and sub-soils. DCB and OX extracted almost similar Al concentrations, suggesting significant Al present in SRO, while DCB extracted Al that was substituted for Fe in the structure of Fe oxides. Crystalline Fe oxides (i.e., goethite and hematite) were dominant in both topsoils and subsoils. Poorly crystalline and SRO alumino-silicate minerals were absent in the soils.

The C:M molar ratio > 6.0 in the PP extracts suggested the co-precipitation of OC with metals by forming Fe/Al complexes, while C:M molar ratio of about 1.5 in the OX fraction indicated both adsorption and co-precipitation processes in the OC association with SRO of Fe and Al. In contrast, the C:M molar ratio ≤ 1 in the DCB fraction suggested that OC was adsorbed on to crystalline Fe/Al oxides possibly forming inner-sphere complexes. Our results show that despite of some non-selectivity and over-lapping dissolution, extraction procedures have potential to routinely determine the role of different forms of Fe and Al in stabilising OC in soils, particularly for large sample sets.

Appendix

Table A1. Dataset of extractable metal(loid)s used for this study

Location	Depth	Fe_{OX} (g/kg)	Fe_{DCB} (g/kg)	Fe_{PP} (g/kg)	Al_{OX} (g/kg)	Al_{DCB} (g/kg)	Al_{PP} (g/kg)	Mn_{OX} (g/kg)	Mn_{DCB} (g/kg)	Mn_{PP} (g/kg)	Si_{OX} (g/kg)	Si_{DCB} (g/kg)	Si_{PP} (g/kg)
Westwood (Cobbitty)	0-20cm	6.50	38.00	4.37	1.65	3.33	1.30	0.87	1.15	0.68	0.29	1.27	0.48
Westwood (Cobbitty)	0-20cm	6.92	37.74	3.86	1.76	3.35	1.19	0.91	1.14	0.62	0.27	1.33	0.32
Westwood (Cobbitty)	20-40cm	5.17	51.37	3.13	2.72	5.28	1.70	0.22	0.37	0.11	0.31	1.26	0.19
Westwood (Cobbitty)	20-40cm	5.12	49.98	4.13	2.64	5.43	2.25	0.21	0.36	0.14	0.25	1.32	0.24
Landsdowne (Cobbitty)	0-20cm	5.32	25.89	1.00	1.52	2.50	0.57	2.64	2.89	0.36	0.44	0.91	0.27
Landsdowne (Cobbitty)	0-20cm	5.38	24.80	1.28	1.58	2.32	0.76	2.53	2.76	0.44	0.34	0.93	0.39
Landsdowne (Cobbitty)	20-40cm	6.76	35.47	0.82	2.39	3.58	0.89	2.89	3.11	0.31	0.68	1.67	0.59
Landsdowne (Cobbitty)	20-40cm	6.86	39.78	0.70	2.46	3.92	0.77	2.93	3.62	0.26	0.70	1.86	0.49
Narrabri (W2)	0-20cm	1.81	8.25	1.05	3.07	1.94	2.63	0.22	0.13	0.16	0.19	0.40	0.70
Narrabri (W2)	0-20cm	1.74	14.78	1.23	3.25	3.37	3.04	0.21	0.23	0.18	0.20	0.90	0.78
Narrabri (W2)	20-40cm	1.65	15.35	0.79	2.54	2.83	2.05	0.04	0.05	0.03	0.25	0.94	0.67
Narrabri (W2)	20-40cm	1.60	16.40	0.81	2.55	3.05	2.20	0.04	0.05	0.03	0.25	1.06	0.52
Nowley (L Paddock)	0-20cm	1.02	9.04	0.70	0.34	0.94	0.31	0.11	0.12	0.09	0.05	0.91	0.45
Nowley (L Paddock)	0-20cm	0.97	9.36	0.67	0.39	0.95	0.32	0.10	0.13	0.10	0.12	0.99	0.39
Nowley (L Paddock)	20-40cm	1.34	61.19	0.02	2.73	10.26	0.60	0.00	0.03	0.00	1.27	2.96	0.22
Nowley (L Paddock)	20-40cm	1.30	59.04	0.03	2.74	9.81	0.69	0.00	0.03	0.00	1.21	2.74	0.41
Kiama	0-20cm	10.19	24.43	2.78	3.34	2.78	1.03	0.65	0.72	0.40	1.64	2.38	0.84
Kiama	0-20cm	10.57	23.00	2.89	3.33	2.73	2.38	0.67	0.70	0.43	1.74	2.36	0.89
Kiama	20-40cm	11.17	29.55	2.03	3.28	3.32	0.85	0.56	0.68	0.24	1.48	2.65	0.70
Kiama	20-40cm	10.10	28.62	1.97	3.23	3.10	0.82	0.54	0.65	0.24	1.52	2.40	0.84
Braidwood	0-20cm	1.76	21.33	0.45	1.25	3.29	0.64	0.04	0.06	0.01	0.47	1.48	0.48
Braidwood	0-20cm	1.82	17.08	0.46	1.32	2.82	0.66	0.03	0.05	0.01	0.47	1.30	0.42
Braidwood	20-40cm	1.32	8.96	0.75	1.48	1.70	0.75	0.10	0.07	0.04	0.47	0.74	0.50
Braidwood	20-40cm	1.38	9.16	0.84	1.53	1.75	0.74	0.10	0.07	0.04	0.40	0.68	0.47
Cooma 1	0-20cm	4.02	26.73	0.68	3.96	3.77	1.18	0.23	0.23	0.13	1.08	1.89	0.65

Cooma 1	0-20cm	4.09	22.56	0.68	3.93	3.13	1.11	0.23	0.19	0.14	1.21	1.45	0.63
Cooma 1	20-40cm	3.14	17.80	0.40	4.04	3.48	1.30	0.02	0.02	0.01	1.02	1.36	0.48
Cooma 1	20-40cm	3.18	18.74	0.39	4.10	3.67	1.35	0.01	0.02	0.01	1.06	1.38	0.55
Cooma 2	0-20cm	7.54	19.32	0.63	3.03	1.62	0.88	0.60	0.39	0.24	1.97	1.27	0.55
Cooma 2	0-20cm	7.04	18.02	0.62	2.94	1.46	0.85	0.59	0.36	0.24	1.99	1.50	0.68
Cooma 2	20-40cm	8.33	17.37	0.50	4.14	1.67	0.94	0.62	0.35	0.13	2.56	1.44	0.55
Cooma 2	20-40cm	8.02	21.04	0.50	3.76	2.24	1.02	0.59	0.43	0.13	2.40	1.73	0.67
Coolringdon	0-20cm	4.19	21.00	0.90	1.55	2.47	0.69	1.40	1.84	0.43	0.40	2.78	0.75
Coolringdon	0-20cm	4.13	20.09	1.01	1.45	2.31	0.81	1.46	1.78	0.45	0.42	2.69	0.85
Coolringdon	20-40cm	4.99	21.04	1.09	3.32	3.08	0.96	0.46	0.32	0.07	0.98	1.56	0.39
Coolringdon	20-40cm	5.02	22.87	1.08	3.19	3.47	0.97	0.44	0.35	0.07	0.90	1.81	0.51
Batlow	0-20cm	3.35	11.29	2.04	3.02	2.56	1.97	0.35	0.27	0.31	0.45	0.76	0.99
Batlow	0-20cm	3.32	10.25	2.03	3.12	2.37	2.07	0.35	0.24	0.32	0.43	0.83	0.54
Batlow	20-40cm	4.04	16.76	1.06	4.84	3.73	2.25	0.14	0.11	0.08	0.76	1.08	0.61
Batlow	20-40cm	4.11	16.06	1.01	4.74	3.46	2.08	0.14	0.10	0.07	0.85	0.96	0.59
Tumbarumba	0-20cm	7.75	42.34	0.74	7.60	5.77	2.65	0.05	0.08	0.02	1.17	1.00	0.34
Tumbarumba	0-20cm	7.63	41.07	0.67	7.15	5.52	2.66	0.05	0.08	0.02	1.10	0.93	0.36
Tumbarumba	20-40cm	7.37	38.90	0.20	7.74	6.09	2.44	0.02	0.06	0.00	1.38	1.03	0.36
Tumbarumba	20-40cm	7.38	39.19	0.18	7.58	5.93	2.43	0.02	0.05	0.00	1.33	1.03	0.30
Wagga Wagga	0-20cm	1.71	12.61	0.43	1.58	1.26	0.88	0.30	0.20	0.22	0.41	1.17	0.78
Wagga Wagga	0-20cm	1.78	13.05	0.46	1.65	1.25	0.99	0.31	0.20	0.25	0.40	1.20	0.94
Wagga Wagga	20-40cm	1.57	17.32	0.20	1.89	1.51	0.77	0.19	0.14	0.12	0.59	1.41	0.97
Wagga Wagga	20-40cm	1.61	18.54	0.16	1.91	1.63	0.71	0.19	0.15	0.10	0.65	1.49	0.86
Sandigo (Narrandera)	0-20cm	2.19	13.59	0.67	2.14	1.49	1.35	0.16	0.12	0.15	0.49	1.40	0.96
Sandigo (Narrandera)	0-20cm	1.82	12.99	0.65	1.77	1.41	1.34	0.13	0.12	0.14	0.38	1.31	1.05
Sandigo (Narrandera)	20-40cm	2.82	19.01	0.82	3.70	3.05	2.27	0.03	0.04	0.03	0.56	1.09	0.79
Sandigo (Narrandera)	20-40cm	2.92	17.24	0.83	3.77	2.86	2.18	0.03	0.03	0.03	0.61	1.09	0.80
Boree Creek	0-20cm	1.96	7.53	1.01	1.38	0.81	1.15	0.43	0.25	0.26	0.29	1.22	1.42
Boree Creek	0-20cm	2.01	7.75	0.60	1.40	0.78	0.69	0.45	0.25	0.16	0.34	1.17	0.94
Boree Creek	20-40cm	1.25	18.55	0.48	1.15	1.49	0.70	0.29	0.32	0.09	0.65	4.07	1.73

Boree Creek	20-40cm	1.23	17.39	0.51	1.20	1.51	0.73	0.31	0.31	0.09	0.61	4.35	1.70
Grabben Gullen	0-20cm	2.85	29.77	0.91	3.06	4.67	1.85	0.06	0.08	0.05	0.46	2.09	0.86
Grabben Gullen	0-20cm	2.85	28.55	0.89	2.99	4.61	1.90	0.06	0.08	0.04	0.46	2.04	0.83
Grabben Gullen	20-40cm	2.61	31.90	0.89	3.18	4.92	2.09	0.04	0.06	0.03	0.38	1.89	0.61
Grabben Gullen	20-40cm	2.51	34.55	0.79	3.02	5.51	1.94	0.03	0.06	0.03	0.38	2.15	0.58
Crookwell	0-20cm	2.99	16.74	1.70	3.44	3.62	2.44	0.03	0.03	0.02	0.31	1.09	0.61
Crookwell	0-20cm	3.01	15.96	1.61	3.36	3.28	2.29	0.03	0.03	0.02	0.33	1.00	0.57
Crookwell	20-40cm	3.43	20.57	1.11	4.03	4.34	2.12	0.00	0.01	0.00	0.56	1.31	0.47
Crookwell	20-40cm	3.38	21.28	1.10	4.05	4.38	2.20	0.00	0.01	0.00	0.62	1.31	0.55
Bathurst 1	0-20cm	0.78	3.42	0.35	0.80	0.38	0.46	0.98	0.57	0.55	0.22	0.52	0.66
Bathurst 1	0-20cm	0.76	3.10	0.35	0.71	0.34	0.47	0.96	0.53	0.57	0.23	0.45	0.69
Bathurst 1	20-40cm	0.73	3.20	0.18	0.82	0.32	0.37	0.64	0.32	0.21	0.29	0.43	0.64
Bathurst 1	20-40cm	0.68	3.09	0.19	0.73	0.28	0.37	0.59	0.30	0.20	0.30	0.42	0.61
Bathurst 2	0-20cm	1.20	2.94	1.04	0.92	0.58	0.88	0.35	0.19	0.33	0.12	0.52	0.90
Bathurst 2	0-20cm	1.14	2.92	1.00	0.83	0.55	0.88	0.33	0.18	0.31	0.09	0.51	0.78
Bathurst 2	20-40cm	1.04	4.94	0.45	1.53	1.10	0.60	0.05	0.04	0.03	0.30	0.92	0.52
Bathurst 2	20-40cm	0.98	5.29	0.41	1.42	1.21	0.60	0.05	0.04	0.03	0.28	1.07	0.49
Molong 1	0-20cm	3.34	21.73	0.58	1.34	1.67	0.55	1.75	1.25	0.52	0.47	1.51	0.76
Molong 1	0-20cm	3.54	19.85	0.57	1.37	1.67	0.60	1.91	1.18	0.52	0.57	1.55	0.78
Molong 1	20-40cm	4.84	21.00	0.63	2.96	2.40	0.85	2.00	1.27	0.33	1.17	2.49	0.81
Molong 1	20-40cm	5.00	20.14	0.58	2.99	2.51	0.80	2.01	1.21	0.33	1.17	2.38	0.82
Molong 2	0-20cm	5.78	32.23	0.62	3.18	2.38	0.80	0.90	0.59	0.28	1.36	2.36	0.99
Molong 2	0-20cm	5.73	33.00	0.54	3.22	2.43	0.74	0.90	0.61	0.25	1.35	2.57	0.80
Molong 2	20-40cm	5.91	36.40	0.46	4.06	3.19	0.85	0.48	0.33	0.13	1.30	2.00	0.59
Molong 2	20-40cm	5.82	37.69	0.53	4.05	3.24	0.89	0.48	0.35	0.14	1.36	2.08	0.70
Wellington	0-20cm	2.72	24.79	0.20	3.20	1.71	0.65	0.60	0.37	0.24	1.74	2.37	1.33
Wellington	0-20cm	2.77	26.64	0.19	3.34	1.90	0.70	0.62	0.41	0.24	1.76	2.52	1.15
Wellington	20-40cm	2.39	25.43	0.11	1.83	1.47	0.40	1.04	0.63	0.25	1.00	1.89	0.80
Wellington	20-40cm	2.41	29.00	0.11	2.05	1.56	0.40	1.06	0.74	0.25	0.95	2.13	0.84
Dunedoo	0-20cm	3.06	33.07	0.23	2.35	2.60	0.42	1.13	0.87	0.20	0.99	2.97	0.72

https://doi.org/10.5194/egusphere-2026-2843
Preprint. Discussion started: 25 August 2026

Dunedoo	0-20cm	3.21	26.12	0.22	2.35	1.95	0.46	1.13	0.67	0.20	0.89	2.21	0.65
Dunedoo	20-40cm	3.22	24.71	0.16	2.44	2.14	0.42	1.20	0.67	0.16	1.12	2.14	0.52
Dunedoo	20-40cm	3.29	24.61	0.16	2.43	2.02	0.46	1.22	0.66	0.16	1.08	2.03	0.63
Mount Wilson	0-20cm	2.62	14.60	1.70	3.18	3.62	2.24	0.06	0.04	0.04	0.24	0.78	0.47
Mount Wilson	0-20cm	2.91	15.09	1.67	3.41	3.81	2.18	0.06	0.04	0.04	0.34	0.76	0.51
Mount Wilson	20-40cm	1.25	15.90	0.90	2.24	4.25	1.46	0.02	0.03	0.01	0.30	0.71	0.42
Mount Wilson	20-40cm	1.32	16.94	0.87	2.30	4.31	1.46	0.02	0.03	0.01	0.37	0.76	0.48
Mount Tomah	0-20cm	8.61	14.36	4.54	6.46	3.26	5.02	0.25	0.12	0.16	0.94	0.88	1.07
Mount Tomah	0-20cm	8.66	17.71	4.15	6.74	4.00	4.43	0.26	0.14	0.14	0.89	0.96	0.97
Mount Tomah	20-40cm	8.88	16.73	5.63	8.00	5.15	6.31	0.28	0.14	0.14	0.70	0.74	1.03
Mount Tomah	20-40cm	8.71	21.96	5.80	7.73	6.11	6.47	0.26	0.19	0.15	0.67	0.99	1.10
Condobolin	0-20cm	4.02	14.30	0.99	2.09	1.63	0.58	0.22	0.16	0.16	0.84	1.60	0.64
Condobolin	0-20cm	3.60	12.95	0.98	1.84	1.40	0.61	0.21	0.15	0.17	0.84	1.49	0.64
Condobolin	20-40cm	2.90	10.99	0.97	1.64	1.26	0.77	0.03	0.03	0.02	0.36	1.17	0.60
Condobolin	20-40cm	2.96	10.70	1.00	1.66	1.18	0.83	0.03	0.03	0.02	0.43	1.21	0.58
Narromine	0-20cm	2.22	8.58	1.29	1.29	0.89	1.17	0.36	0.19	0.27	0.31	1.38	1.50
Narromine	0-20cm	2.11	7.58	1.17	1.20	0.72	1.07	0.34	0.17	0.27	0.26	1.11	1.26
Narromine	20-40cm	1.67	7.66	1.69	1.15	0.83	1.40	0.12	0.07	0.08	0.32	2.36	2.45
Narromine	20-40cm	1.64	7.91	1.43	1.11	0.89	1.16	0.11	0.07	0.08	0.25	2.56	1.99
Coonabarabran	0-20cm	1.74	12.86	0.29	3.48	2.75	1.21	0.08	0.05	0.05	0.72	1.34	0.63
Coonabarabran	0-20cm	1.56	14.10	0.28	3.24	2.91	1.24	0.07	0.06	0.05	0.58	1.46	0.78
Coonabarabran	20-40cm	1.49	11.04	0.27	3.54	2.79	1.25	0.05	0.04	0.04	0.67	1.33	0.63
Coonabarabran	20-40cm	1.38	12.58	0.24	3.45	3.06	1.14	0.05	0.05	0.03	0.65	1.52	0.56
Baradine	0-20cm	1.96	20.18	0.42	2.65	3.13	1.32	0.39	0.32	0.24	0.29	1.31	0.35
Baradine	0-20cm	2.10	15.51	0.41	2.76	2.40	1.29	0.41	0.24	0.23	0.27	0.90	0.49
Baradine	20-40cm	1.47	20.53	0.17	2.02	2.66	0.81	0.10	0.10	0.06	0.29	1.18	0.36
Baradine	20-40cm	1.41	16.42	0.19	2.00	2.08	0.93	0.09	0.08	0.06	0.36	0.97	0.38
The Pilliga	0-20cm	3.04	15.25	0.95	1.76	1.58	1.10	1.10	0.65	0.60	0.19	1.27	0.63
The Pilliga	0-20cm	3.16	14.00	1.03	1.81	1.36	1.16	1.17	0.62	0.65	0.24	1.17	0.73
The Pilliga	20-40cm	3.75	18.40	1.04	1.24	1.13	0.79	0.84	0.51	0.36	0.43	1.60	1.01

https://doi.org/10.5194/egusphere-2026-2843
Preprint. Discussion started: 25 August 2026

The Pilliga	20-40cm	3.83	19.10	0.77	1.28	1.25	0.62	0.85	0.53	0.32	0.48	1.62	0.76
Inverell	0-20cm	12.81	56.63	0.85	5.54	5.72	0.95	1.91	1.25	0.47	2.14	3.17	0.77
Inverell	0-20cm	12.77	56.76	0.86	5.66	5.74	0.97	1.99	1.25	0.49	2.16	2.96	0.82
Inverell	20-40cm	11.13	47.40	0.56	6.34	5.28	0.92	1.76	1.10	0.18	2.92	3.92	1.14
Inverell	20-40cm	11.04	51.45	0.65	6.03	5.75	1.05	1.62	1.19	0.20	3.03	4.17	1.35
Tabulam	0-20cm	4.85	60.40	0.91	4.66	6.64	2.99	0.02	0.04	0.01	0.49	2.60	0.42
Tabulam	0-20cm	4.85	44.82	0.84	4.39	5.07	2.76	0.02	0.03	0.01	0.58	2.06	0.38
Tabulam	20-40cm	2.70	14.93	0.31	4.46	3.08	2.22	0.00	0.01	0.00	0.32	3.24	0.26
Tabulam	20-40cm	2.70	14.64	0.34	4.55	3.04	2.41	0.00	0.01	0.00	0.33	3.24	0.42
Clovass	0-20cm	5.53	25.60	0.77	6.82	5.12	1.35	0.09	0.08	0.01	1.32	2.76	0.58
Clovass	0-20cm	5.53	23.66	0.77	6.67	4.52	1.39	0.09	0.07	0.01	1.25	2.36	0.46
Clovass	20-40cm	5.96	35.42	0.59	6.54	4.86	1.31	0.10	0.10	0.01	1.50	2.91	0.60
Clovass	20-40cm	5.93	33.16	0.61	6.69	4.74	1.31	0.10	0.09	0.01	1.48	2.75	0.56
Casino	0-20cm	4.22	33.67	1.09	5.66	6.41	2.96	0.03	0.04	0.01	0.53	1.55	0.33
Casino	0-20cm	4.46	32.72	1.14	5.98	6.34	3.04	0.03	0.04	0.01	0.61	1.55	0.45
Casino	20-40cm	5.07	29.93	0.28	6.17	4.16	3.08	0.01	0.01	0.00	0.51	1.93	0.33
Casino	20-40cm	5.18	41.50	0.31	6.32	5.97	3.26	0.01	0.02	0.00	0.55	2.65	0.33
Guyra	0-20cm	10.39	71.71	1.99	4.64	6.60	1.69	2.90	1.48	1.07	1.06	2.08	0.71
Guyra	0-20cm	9.45	74.04	1.84	4.26	7.03	1.53	2.66	1.57	0.97	1.01	2.07	0.80
Guyra	20-40cm	8.00	79.87	0.73	5.39	9.80	1.14	1.14	0.91	0.26	1.07	2.04	0.35
Guyra	20-40cm	7.93	72.09	0.74	5.13	9.35	1.28	1.13	0.84	0.27	0.99	1.75	0.39
Armidale	0-20cm	5.51	59.70	0.65	4.79	6.08	1.26	0.95	0.64	0.44	1.02	1.99	0.61
Armidale	0-20cm	5.50	61.44	0.71	5.06	6.26	1.29	0.99	0.65	0.46	1.07	1.95	0.64
Armidale	20-40cm	5.87	62.08	0.72	3.78	5.78	1.06	1.04	0.71	0.47	0.63	1.61	0.42
Armidale	20-40cm	6.14	66.11	0.70	4.11	6.24	0.99	1.13	0.77	0.45	0.72	1.65	0.41
Murrurundi	0-20cm	2.68	20.00	0.30	1.78	1.97	0.38	0.08	0.08	0.03	0.57	1.90	0.39
Murrurundi	0-20cm	2.65	22.95	0.30	1.71	2.37	0.34	0.08	0.09	0.03	0.54	2.36	0.38
Murrurundi	20-40cm	2.25	22.58	0.17	1.60	2.28	0.27	0.13	0.16	0.03	0.79	3.13	0.59
Murrurundi	20-40cm	2.22	18.09	0.20	1.59	1.79	0.33	0.12	0.13	0.03	0.70	2.47	0.61
Somersby	0-20cm	1.90	11.52	1.41	3.05	3.13	2.28	0.02	0.01	0.01	0.08	0.41	0.46

https://doi.org/10.5194/egusphere-2026-2843
Preprint. Discussion started: 25 August 2026

Somersby	0-20cm	1.66	8.73	1.42	2.59	2.29	2.30	0.01	0.01	0.01	0.11	0.27	0.45
Somersby	20-40cm	0.91	11.55	0.90	1.98	3.02	1.87	0.00	0.01	0.00	0.15	0.28	0.32
Somersby	20-40cm	0.93	12.04	0.87	2.02	3.23	1.83	0.00	0.01	0.00	0.12	0.30	0.30

https://doi.org/10.5194/egusphere-2026-2843
Preprint. Discussion started: 25 August 2026

767 Table A2. Dataset of extractable carbon (C) used for this study

Location	Depth	C_{OX} (g/kg)	C_{DCB} (g/kg)	C_{PP} (g/kg)
Westwood (Cobbitty)	0-20cm	21.20	24.50	26.06
Westwood (Cobbitty)	20-40cm	26.48	27.46	30.52
Landsdowne (Cobbitty)	0-20cm	26.35	28.42	31.01
Landsdowne (Cobbitty)	20-40cm	24.52	26.62	29.01
Narrabri (W2)	0-20cm	10.57	20.87	21.44
Narrabri (W2)	20-40cm	6.17	8.74	13.08
Nowley (L Paddock)	0-20cm	2.26	2.85	3.32
Nowley (L Paddock)	20-40cm	4.94	3.38	7.67
Kiama	0-20cm	10.06	27.74	29.88
Kiama	20-40cm	13.82	19.23	23.66
Braidwood	0-20cm	23.19	23.50	23.05
Braidwood	20-40cm	21.28	21.78	22.89
Cooma 1	0-20cm	17.39	17.64	23.16
Cooma 1	20-40cm	17.04	16.11	19.77
Cooma 2	0-20cm	9.65	13.00	15.74
Cooma 2	20-40cm	7.25	11.32	13.43
Coolringdon	0-20cm	7.26	10.46	14.24
Coolringdon	20-40cm	5.39	7.63	12.71
Batlow	0-20cm	5.68	6.23	9.93
Batlow	20-40cm	2.10	4.99	6.99
Tumbarumba	0-20cm	6.25	10.48	14.18
Tumbarumba	20-40cm	9.83	13.81	15.90
Wagga Wagga	0-20cm	1.60	4.39	8.01
Wagga Wagga	20-40cm	1.66	5.30	7.27
Sandigo (Narrandera)	0-20cm	1.16	4.48	9.31
Sandigo (Narrandera)	20-40cm	1.48	2.84	7.89
Boree Creek	0-20cm	0.92	3.27	7.43
Boree Creek	20-40cm	5.67	7.27	10.50
Grabben Gullen	0-20cm	2.32	4.68	10.24
Grabben Gullen	20-40cm	2.29	3.93	8.72
Crookwell	0-20cm	1.83	5.78	9.82
Crookwell	20-40cm	2.41	4.33	6.94
Bathurst 1	0-20cm	0.66	1.46	3.63
Bathurst 1	20-40cm	0.82	1.46	3.11
Bathurst 2	0-20cm	2.81	5.62	8.86
Bathurst 2	20-40cm	5.15	6.62	7.89
Molong 1	0-20cm	1.18	3.56	6.86
Molong 1	20-40cm	0.71	3.25	7.99
Molong 2	0-20cm	1.05	2.96	8.24
Molong 2	20-40cm	1.87	7.55	12.11
Wellington	0-20cm	10.83	14.27	18.59
Wellington	20-40cm	7.95	12.64	18.27
Dunedoo	0-20cm	12.46	15.96	20.15
Dunedoo	20-40cm	11.35	15.48	19.84

https://doi.org/10.5194/egusphere-2026-2843
Preprint. Discussion started: 25 August 2026

Mount Wilson	0-20cm	6.75	9.04	13.48
Mount Wilson	20-40cm	9.73	10.36	12.22
Mount Tomah	0-20cm	9.04	15.96	20.42
Mount Tomah	20-40cm	8.39	12.24	20.98
Condobolin	0-20cm	10.66	14.57	19.40
Condobolin	20-40cm	10.05	12.81	15.47
Narromine	0-20cm	6.83	10.54	14.77
Narromine	20-40cm	4.12	6.46	9.60
Coonabarabran	0-20cm	1.48	4.28	8.10
Coonabarabran	20-40cm	1.91	3.38	6.92
Baradine	0-20cm	0.77	3.10	7.37
Baradine	20-40cm	1.52	3.89	5.09
The Pilliga	0-20cm	1.91	4.43	8.80
The Pilliga	20-40cm	1.37	3.18	4.94
Inverell	0-20cm	1.97	8.98	13.46
Inverell	20-40cm	3.00	6.89	11.64
Tabulam	0-20cm	5.32	8.80	11.43
Tabulam	20-40cm	3.72	5.15	8.74
Clovass	0-20cm	3.91	3.48	9.65
Clovass	20-40cm	1.01	4.94	8.65
Casino	0-20cm	2.73	5.03	8.50
Casino	20-40cm	1.79	4.05	7.46
Guyra	0-20cm	3.08	6.72	12.32
Guyra	20-40cm	1.43	4.84	8.67
Armidale	0-20cm	3.08	3.05	10.21
Armidale	20-40cm	1.18	2.18	8.31
Murrurundi	0-20cm	1.84	0.60	5.19
Murrurundi	20-40cm	1.59	0.48	4.26
Somersby	0-20cm	2.31	10.62	7.16
Somersby	20-40cm	0.52	3.56	2.76

Author contribution

BEA: Conceptualization, Data curation, Formal analysis, Investigation, Methodology, Software, Validation, Project administration, Visualization and Writing (original draft preparation). FAD and CW: Supervision, Funding acquisition and writing (review and editing). BS: Conceptualization, Funding acquisition, Methodology, Supervision and Writing (review and editing).

Data availability

The raw data used for this study is available in Tables A1 and A2 in the appendix.

Competing interests

The authors declare that they have no conflict of interest.

https://doi.org/10.5194/egusphere-2026-2843
Preprint. Discussion started: 25 August 2026

Acknowledgements

We acknowledge the **Soil Science Challenge Grants Program** funded by the **Australian Government Department of Agriculture, Fisheries and Forestry** and this article contributes towards the **National Soil Strategy** and the implementation of the **National Soil Action Plan**. Bright is thankful to the Tertiary Education Trust Fund (TETFund), Nigeria for the financial support in tuition fees and living expenses.

References

Amenkhienan, B.E., Dijkstra, F., Warren, C., Singh, B., Understanding extractable metal species relationships with phosphorus sorption and organic carbon in soils. Soil Res., 62, https://doi.org/10.1071/sr24118., 2024.

Ashida, K., Watanabe, T., Urayama, S., Hartono, A., Kilasara, M., Ze, A.D.M., Nakao, A., Sugihara, S., Funakawa, S., Quantitative relationship between organic carbon and geochemical properties in tropical surface and subsurface soils. Biogeochem., 155, 77-95, https://doi.org/10.1007/s10533-021-00813-8, 2021.

Baldock, J.A., Skjemstad, J.O., Role of the soil matrix and minerals in protecting natural organic materials against biological attack. Org. Geochem., 31, 697-710, https://doi.org/10.1016/S0146-6380(00)00049-8, 2000.

Bascomb, C.L., Distribution of Pyrophosphate-Extractable Iron and Organic Carbon in Soils of Various Groups. J. Soil Sci., 19, 251-268, https://doi.org/10.1111/j.1365-2389.1968.tb01538.x, 1968.

Batjes, N.H., Total carbon and nitrogen in the soils of the world. Eur. J. Soil Sci., 65, 10-21, https://doi.org/10.1111/ejss.12114_2, 2014.

Bigham, J., Golden, D., Bowen, L., Buol, S., Weed, S., Iron Oxide Mineralogy of Well-drained Ultisols and Oxisols: I. Characterization of Iron Oxides in Soil Clays by Mössbauer Spectroscopy, X-ray Diffractometry, and Selected Chemical Techniques. Soil Sci. Soc. Am. J., 42, 816-825, 1978.

Borggaard, O.K., Phase identification by selective dissolution techniques. Iron in Soils and Clay Minerals. Springer, 83-98. 1988.

Carlson, L., Schwertmann, U., Natural Ferrihydrites in Surface Deposits from Finland and Their Association with Silica. Geochim. Cosmochim. Acta, 45, 421-429, https://doi.org/10.1016/0016-7037(81)90250-7, 1981.

Chadwick, O.A., Chorover, J., The chemistry of pedogenic thresholds. *Geoderma,* **100**, 321-353, https://doi.org/10.1016/S0016-7061(01)00027-1, 2001.

Chao, T.T., Zhou, L., Extraction Techniques for Selective Dissolution of Amorphous Iron-Oxides from Soils and Sediments. Soil Sci. Soc. Am. J., 47, 225-232, https://doi.org/10.2136/sssaj1983.03615995004700020010x, 1983.

Chen, C., Dynes, J.J., Wang, J., Sparks, D.L., Properties of Fe-organic matter associations via coprecipitation versus adsorption. Environ. Sci. Technol., 48, 13751-13759, https://doi.org/10.1021/es503669u, 2014.

Chen, C., Hall, S.J., Coward, E., Thompson, A., Iron-mediated organic matter decomposition in humid soils can counteract protection. Nat. Commun., 11, 2255, https://doi.org/10.1038/s41467-020-16071-5, 2020.

Childs, C., Wilson, A., Iron oxide minerals in soils of the Ha'apai group, Kingdom of Tonga. Soil Res., 21, 489-503, 1983.

Christensen, B.T., Physical fractionation of soil and organic matter in primary particle size and density separates. Adv. Soil Sci., 20, 1-90, 1992.

Colombo, C., Torrent, J., Relationships between Aggregation and Iron-Oxides in Terra Rossa Soils from Southern Italy. Catena, 18, 51-59, https://doi.org/10.1016/0341-8162(91)90006-J, 1991.

Cornell, R.M., Schwertmann, U., The iron oxides: structure, properties, reactions, occurrences, and uses. Wiley-vch Weinheim, 2003.

https://doi.org/10.5194/egusphere-2026-2843
Preprint. Discussion started: 25 August 2026

Coward, E.K., Ohno, T., Plante, A.F., Adsorption and Molecular Fractionation of Dissolved Organic Matter on Iron-Bearing Mineral Matrices of Varying Crystallinity. Environ. Sci. Technol., 52, 1036-1044, https://doi.org/10.1021/acs.est.7b04953, 2018.

Coward, E.K., Thompson, A.T., Plante, A.F., Iron-mediated mineralogical control of organic matter accumulation in tropical soils. Geoderma, 306, 206-216, https://doi.org/10.1016/j.geoderma.2017.07.026, 2017.

Crowther, T.W., Todd-Brown, K.E., Rowe, C.W., Wieder, W.R., Carey, J.C., Machmuller, M.B., Snoek, B.L., Fang, S., Zhou, G., Allison, S.D., Blair, J.M., Bridgham, S.D., Burton, A.J., Carrillo, Y., Reich, P.B., Clark, J.S., Classen, A.T., Dijkstra, F.A., Elberling, B., Emmett, B.A., Estiarte, M., Frey, S.D., Guo, J., Harte, J., Jiang, L., Johnson, B.R., Kroel-Dulay, G., Larsen, K.S., Laudon, H., Lavallee, J.M., Luo, Y., Lupascu, M., Ma, L.N., Marhan, S., Michelsen, A., Mohan, J., Niu, S., Pendall, E., Penuelas, J., Pfeifer-Meister, L., Poll, C., Reinsch, S., Reynolds, L.L., Schmidt, I.K., Sistla, S., Sokol, N.W., Templer, P.H., Treseder, K.K., Welker, J.M., Bradford, M.A., Quantifying global soil carbon losses in response to warming. Nat., 540, 104-108, https://doi.org/10.1038/nature20150, 2016.

Dahlgren, R.A., Quantification of allophane and imogolite. In: J.E. Amonette, J.W. Stucki (Eds.), Quantitative Methods in Soil Mineralogy. Soil Sci. Soc. Am., 430-451. 1994.

Daly, B., Identification of podzols and podzolised soils in New Zealand by relative absorbance of oxalate extracts of A and B horizons. Geoderma, 28, 29-38, 1982.

Davey, B.G., Russell, J.D., Wilson, M.J., Iron-Oxide and Clay-Minerals and Their Relation to Colors of Red and Yellow Podzolic Soils near Sydney, Australia. Geoderma, 14, 125-138, https://doi.org/10.1016/0016-7061(75)90071-3, 1975.

Estes, E.R., Andeer, P.F., Nordlund, D., Wankel, S.D., Hansel, C.M., Biogenic manganese oxides as reservoirs of organic carbon and proteins in terrestrial and marine environments. Geobiol., 15, 158-172, https://doi.org/10.1111/gbi.12195, 2017.

Eusterhues, K., Hädrich, A., Neidhardt, J., Küsel, K., Keller, T.F., Jandt, K.D., Totsche, K.U., Reduction of ferrihydrite with adsorbed and coprecipitated organic matter: microbial reduction by vs. abiotic reduction by Na-dithionite. Biogeosci., 11, 4953-4966, https://doi.org/10.5194/bg-11-4953-2014, 2014.

Eusterhues, K., Rennert, T., Knicker, H., Kogel-Knabner, I., Totsche, K.U., Schwertmann, U., Fractionation of organic matter due to reaction with ferrihydrite: coprecipitation versus adsorption. Environ. Sci. Technol., 45, 527-533, https://doi.org/10.1021/es1023898, 2011.

Evans, L.J., Smillie, G.W., Extractable Iron and Aluminum and Their Relationship to Phosphate Retention in Irish Soils. Ir. J. Agric. Res., 15, 65-73, 1976.

Farmer, V.C., Russell, J.D., Smith, B.F.L., Extraction of Inorganic Forms of Translocated Al, Fe and Si from a Podzol Bs Horizon. J. Soil Sci., 34, 571-576, https://doi.org/10.1111/j.1365-2389.1983.tb01056.x, 1983.

Feller, C., Albrecht, A., Tessier, D., Aggregation and organic matter storage in kaolinitic and smectitic tropical soils. Structure and organic matter storage in agricultural soils. CRC Press, 309-359. 2020.

Fitzpatrick, R.W., Schwertmann, U., Al-Substituted Goethite - an Indicator of Pedogenic and Other Weathering Environments in South-Africa. Geoderma, 27, 335-347, https://doi.org/10.1016/0016-7061(82)90022-2, 1982.

Fritzsche, A., Schroder, C., Wieczorek, A.K., Handel, M., Ritschel, T., Totsche, K.U., Structure and composition of Fe-OM co-precipitates that form in soil-derived solutions. Geochim. Cosmochim. Acta, 169, 167-183, https://doi.org/10.1016/j.gca.2015.07.041, 2015.

Gamble, E.E., Daniels, R.B., Iron and Silica in Water, Acid Ammonium Oxalate, and Dithionite Extracts of Some North-Carolina Coastal-Plain Soils. Soil Sci. Soc. Am. J., 36, 939-943, https://doi.org/10.2136/sssaj1972.03615995003600060030x, 1972.

Gee, G.W., Or, D., 2.4 Particle-size analysis. *Methods of soil analysis: part 4 physical methods,* 5, 255-293, 2002.

Gu, B., Schmitt, J., Chen, Z., Liang, L., McCarthy, J.F., Adsorption and desorption of natural organic matter on iron oxide: mechanisms and models. Environ. Sci. Technol., 28, 38-46, https://doi.org/10.1021/es00050a007, 1994.

https://doi.org/10.5194/egusphere-2026-2843
Preprint. Discussion started: 25 August 2026

Guggenberger, G., Kaiser, K., Dissolved organic matter in soil: challenging the paradigm of sorptive preservation. Geoderma, 113, 293-310, https://doi.org/10.1016/S0016-7061(02)00366-X, 2003.
Hall, S.J., Thompson, A., What do relationships between extractable metals and soil organic carbon concentrations mean? Soil Sci. Soc. Am. J., 86, 195-208, https://doi.org/https://doi.org/10.1002/saj2.20343, 2022.
Han, L.F., Sun, K., Keiluweit, M., Yang, Y., Yang, Y., Jin, J., Sun, H.R., Wu, F.C., Xing, B.S., Mobilization of ferrihydrite-associated organic carbon during Fe reduction: Adsorption versus coprecipitation. Chem. Geol., 503, 61-68, https://doi.org/10.1016/j.chemgeo.2018.10.028, 2019.
Hassink, J., The capacity of soils to preserve organic C and N by their association with clay and silt particles. Plant Soil, 191, 77-87, https://doi.org/10.1023/A:1004213929699, 1997.
Heckman, K., Grandy, A.S., Gao, X., Keiluweit, M., Wickings, K., Carpenter, K., Chorover, J., Rasmussen, C., Sorptive fractionation of organic matter and formation of organo-hydroxy-aluminum complexes during litter biodegradation in the presence of gibbsite. Geochim. Cosmochim. Acta, 121, 667-683, https://doi.org/10.1016/j.gca.2013.07.043, 2013.
Heckman, K., Lawrence, C.R., Harden, J.W., A sequential selective dissolution method to quantify storage and stability of organic carbon associated with Al and Fe hydroxide phases. Geoderma, 312, 24-35, https://doi.org/10.1016/j.geoderma.2017.09.043, 2018.
Higashi, T., Characterization of Al/Fe - Humus Complexes in Dystrandepts through Comparison with Synthetic Forms. Geoderma, 31, 277-288, https://doi.org/10.1016/0016-7061(83)90041-1, 1983.
Higashi, T., Deconinck, F., Gelaude, F., Characterization of Some Spodic Horizons of the Campine (Belgium) with Dithionite-Citrate, Pyrophosphate and Sodium Hydroxide-Tetraborate. Geoderma, 25, 131-142, https://doi.org/10.1016/0016-7061(81)90010-0, 1981.
Huang, X.Y., Liu, X.W., Liu, J.L., Chen, H., Iron-bound organic carbon and their determinants in peatlands of China. Geoderma, 391, 114974, https://doi.org/10.1016/j.geoderma.2021.114974, 2021.
Jackson, R.B., Lajtha, K., Crow, S.E., Hugelius, G., Kramer, M.G., Piñeiro, G., The ecology of soil carbon: pools, vulnerabilities, and biotic and abiotic controls. Annu. Rev. Ecol. Evol. Syst., 48, 419-445, https://doi.org/10.1146/annurev-ecolsys-112414-054234, 2017.
Jardine, P.M., Zelazny, L.W., Surface reactions of aqueous aluminum species. The environmental chemistry of aluminum. CRC Press, 221-270. 2020.
Jarvis, S.C., The Forms of Occurrence of Manganese in Some Acidic Soils. J. Soil Sci., 35, 421-429, https://doi.org/10.1111/j.1365-2389.1984.tb00298.x, 1984.
Jeanroy, E., Guillet, B., The occurrence of suspended ferruginous particles in pyrophosphate extracts of some soil horizons. Geoderma, 26, 95-105, https://doi.org/10.1016/0016-7061(81)90078-1, 1981.
Jeewani, P.H., Ling, L., Fu, Y.Y., Van Zwieten, L., Zhu, Z.K., Ge, T.D., Guggenberger, G., Luo, Y., Xu, J.M., The stoichiometric C-Fe ratio regulates glucose mineralization and stabilization via microbial processes. Geoderma, 383, 114769, https://doi.org/10.1016/j.geoderma.2020.114769, 2021.
Jindaluang, W., Kheoruenromne, I., Suddhiprakarn, A., Singh, B.P., Singh, B., Influence of soil texture and mineralogy on organic matter content and composition in physically separated fractions soils of Thailand. Geoderma, 195, 207-219, https://doi.org/10.1016/j.geoderma.2012.12.003, 2013.
Kaiser, K., Sorption of natural organic matter fractions to goethite (α-FeOOH):: effect of chemical composition as revealed by liquid-state C NMR and wet-chemical analysis. Org. Geochem., 34, 1569-1579, https://doi.org/10.1016/S0146-6380(03)00120-7, 2003.
Kaiser, K., Guggenberger, G., The role of DOM sorption to mineral surfaces in the preservation of organic matter in soils. Org. Geochem., 31, 711-725, https://doi.org/10.1016/s0146-6380(00)00046-2, 2000.
Kaiser, K., Guggenberger, G., Mineral surfaces and soil organic matter. Eur. J. Soil Sci., 54, 219-236, https://doi.org/10.1046/j.1365-2389.2003.00544.x, 2003.
Kaiser, K., Mikutta, R., Guggenberger, G., Increased stability of organic matter sorbed to ferrihydrite and goethite on aging. Soil Sci. Soc. Am. J., 71, 711-719, https://doi.org/10.2136/sssaj2006.0189, 2007.
Kaiser, K., Zech, W., Defects in estimation of aluminum in humus complexes of podzolic soils by pyrophosphate extraction. Soil Sci., 161, 452-458, https://doi.org/10.1097/00010694-199607000-00005, 1996.

https://doi.org/10.5194/egusphere-2026-2843
Preprint. Discussion started: 25 August 2026

928 Kalbitz, K., Schwesig, D., Rethemeyer, J., Matzner, E., Stabilization of dissolved organic matter by sorption
929 to the mineral soil. Soil Biol. Biochem., 37, 1319-1331, https://doi.org/10.1016/j.soilbio.2004.11.028,
930 2005.
931 Kleber, M., Eusterhues, K., Keiluweit, M., Mikutta, C., Mikutta, R., Nico, P.S., Mineral-Organic Associations:
932 Formation, Properties, and Relevance in Soil Environments. Adv. Agron., 130, 1-140,
933 https://doi.org/10.1016/bs.agron.2014.10.005, 2015.
934 Kleber, M., Mikutta, R., Torn, M.S., Jahn, R., Poorly crystalline mineral phases protect organic matter in
935 acid subsoil horizons. Eur. J. Soil Sci., 56, 717-725, https://doi.org/10.1111/j.1365-2389.2005.00706.x,
936 2005.
937 Kögel-Knabner, I., Guggenberger, G., Kleber, M., Kandeler, E., Kalbitz, K., Scheu, S., Eusterhues, K.,
938 Leinweber, P., Organo-mineral associations in temperate soils: Integrating biology, mineralogy, and organic
939 matter chemistry. J. Plant Nutr. Soil, 171, 61-82, 2008.
940 Kramer, M.G., Chadwick, O.A., Climate-driven thresholds in reactive mineral retention of soil carbon at the
941 global scale. Nat. Clim. Change, 8, 1104-1108, https://doi.org/10.1038/s41558-018-0341-4, 2018.
942 Laganière, J., Angers, D.A., Paré, D., Carbon accumulation in agricultural soils after afforestation: a meta-
943 analysis. Glob. Chang. Biol., 16, 439-453, https://doi.org/10.1111/j.1365-2486.2009.01930.x, 2010.
944 Lal, R., Soil carbon sequestration impacts on global climate change and food security. Sci, 304, 1623-1627,
945 https://doi.org/10.1126/science.1097396, 2004.
946 Lal, R., Kimble, J.M., Stewart, B.A., Eswaran, H., Global climate change and pedogenic carbonates. 1999.
947 Lalonde, K., Mucci, A., Ouellet, A., Gelinas, Y., Preservation of organic matter in sediments promoted by
948 iron. Nat., 483, 198-200, https://doi.org/10.1038/nature10855, 2012.
949 Lawrence, C.R., Harden, J.W., Xu, X.M., Schulz, M.S., Trumbore, S.E., Long-term controls on soil organic
950 carbon with depth and time: A case study from the Cowlitz River Chronosequence, WA USA. Geoderma,
951 247, 73-87, https://doi.org/10.1016/j.geoderma.2015.02.005, 2015.
952 Lehmann, J., Kleber, M., The contentious nature of soil organic matter. Nat., 528, 60-68,
953 https://doi.org/10.1038/nature16069, 2015.
954 Li, H., Santos, F., Butler, K., Herndon, E., A Critical Review on the Multiple Roles of Manganese in Stabilizing
955 and Destabilizing Soil Organic Matter. Environ. Sci. Technol., 55, 12136-12152,
956 https://doi.org/10.1021/acs.est.1c00299, 2021.
957 Li, Q., Hu, W., Li, L., Li, Y., Interactions between organic matter and Fe oxides at soil micro-interfaces:
958 Quantification, associations, and influencing factors. Sci. Total Environ., 855, 158710,
959 https://doi.org/10.1016/j.scitotenv.2022.158710, 2023.
960 Li, Y., Wang, C.C., Zou, C., Zhao, Y., Wei, P., Liu, Y.Y., Zhao, X.J., Lin, D.M., He, X.J., Huang, J.L., Guo, J.S., Zhu,
961 G.Y., Effects of iron/aluminum mineral phases on soil organic carbon storage in different clay soils of
962 subtropical acidic forests. Catena, 252, 108853, https://doi.org/10.1016/j.catena.2025.108853, 2025.
963 Loeppert, R., Inskeep, K., Methods of Soil Analysis: Part III. Chemical Methods. In: D.L. Sparks, A.L.P., P.A.
964 Helmke, R.H. Loeppert, P.N. Soltanpour, M.A. Tabatabai, C.T. Johnston, M.E. Sumner (Ed.), Soil Science
965 Society of America Book Series. Wiley, Madison, WI, 639-664. https://doi.org/10.2136/sssabookser5.3,
966 1996.
967 Loveland, P.J., Digby, P., The Extraction of Fe and Al by 0.1 M-Pyrophosphate Solutions - a Comparison of
968 Some Techniques. J. Soil Sci., 35, 243-250, https://doi.org/10.1111/j.1365-2389.1984.tb00280.x, 1984.
969 Lützow, M.v., Kögel-Knabner, I., Ekschmitt, K., Matzner, E., Guggenberger, G., Marschner, B., Flessa, H.,
970 Stabilization of organic matter in temperate soils: mechanisms and their relevance under different soil
971 conditions–a review. Eur. J. Soil Sci., 57, 426-445, 2006.
972 Manceau, A., Schlegel, M.L., Musso, M., Sole, V.A., Gauthier, C., Petit, P.E., Trolard, F., Crystal chemistry of
973 trace elements in natural and synthetic goethite. Geochim. Cosmochim. Acta, 64, 3643-3661,
974 https://doi.org/10.1016/S0016-7037(00)00427-0, 2000.
975 Mansfeldt, T., Schuth, S., Häusler, W., Wagner, F.E., Kaufhold, S., Overesch, M., Iron oxide mineralogy and
976 stable iron isotope composition in a Gleysol with petrogleyic properties. J. Soils Sediments, 12, 97-114,
977 https://doi.org/10.1007/s11368-011-0402-z, 2012.

https://doi.org/10.5194/egusphere-2026-2843
Preprint. Discussion started: 25 August 2026

Masiello, C.A., Chadwick, O.A., Southon, J., Torn, M.S., Harden, J.W., Weathering controls on mechanisms of carbon storage in grassland soils - art. no. GB4023. Global Biogeochem. Cy., 18, GB4023, https://doi.org/10.1029/2004gb002219, 2004.
Matus, F., Rumpel, C., Neculman, R., Panichini, M., Mora, M.L., Soil carbon storage and stabilisation in andic soils: A review. Catena, 120, 102-110, https://doi.org/https://doi.org/10.1016/j.catena.2014.04.008, 2014.
McCarthy, J.F., Ilavsky, J., Jastrow, J.D., Mayer, L.M., Perfect, E., Zhuang, J., Protection of organic carbon in soil microaggregates via restructuring of aggregate porosity and filling of pores with accumulating organic matter. Geochim. Cosmochim. Acta, 72, 4725-4744, https://doi.org/10.1016/j.gca.2008.06.015, 2008.
McKeague, J., An evaluation of 0.1 M pyrophosphate and pyrophosphate-dithionite in comparison with oxalate as extractants of the accumulation products in podzols and some other soils. Can. J. Soil Sci., 47, 95-99, 1967.
McKeague, J., Schuppli, P., Changes in concentration of iron and aluminum in pyrophosphate extracts of soil and composition of sediment resulting from ultracentrifugation in relation to spodic horizon criteria. Soil Sci., 134, 265-270, 1982.
Mckeague, J.A., Day, D.H., Dithionite- and Oxalate-Extractable Fe and Al as Aids in Differentiating Various Classes of Soils. Can. J. Soil Sci., 46, 13-+, https://doi.org/10.4141/cjss66-003, 1966.
Mehra, O., Jackson, M., Iron oxide removal from soils and clays by a dithionite–citrate system buffered with sodium bicarbonate. Clays Clay Miner. Elsevier, 317-327. 1960.
Mikutta, C., Wiederhold, J.G., Cirpka, O.A., Hofstetter, T.B., Bourdon, B., Von Gunten, U., Iron isotope fractionation and atom exchange during sorption of ferrous iron to mineral surfaces. Geochim. Cosmochim. Acta, 73, 1795-1812, https://doi.org/10.1016/j.gca.2009.01.014, 2009.
Mikutta, R., Kleber, M., Torn, M.S., Jahn, R., Stabilization of soil organic matter: Association with minerals or chemical recalcitrance? Biogeochem., 77, 25-56, https://doi.org/10.1007/s10533-005-0712-6, 2006.
Mikutta, R., Lorenz, D., Guggenberger, G., Haumaier, L., Freund, A., Properties and reactivity of Fe-organic matter associations formed by coprecipitation adsorption: Clues from arsenate batch adsorption. Geochim. Cosmochim. Acta, 144, 258-276, https://doi.org/10.1016/j.gca.2014.08.026, 2014.
Mikutta, R., Mikutta, C., Kalbitz, K., Scheel, T., Kaiser, K., Jahn, R., Biodegradation of forest floor organic matter bound to minerals via different binding mechanisms. Geochim. Cosmochim. Acta, 71, 2569-2590, https://doi.org/10.1016/j.gca.2007.03.002, 2007.
Mikutta, R., Zang, U., Chorover, J., Haumaier, L., Kalbitz, K., Stabilization of extracellular polymeric substances (*Bacillus subtilis*) by adsorption to and coprecipitation with Al forms. Geochim. Cosmochim. Acta, 75, 3135-3154, https://doi.org/10.1016/j.gca.2011.03.006, 2011.
Mu, C.C., Zhang, T.J., Zhao, Q., Guo, H., Zhong, W., Su, H., Wu, Q.B., Soil organic carbon stabilization by iron in permafrost regions of the Qinghai-Tibet Plateau. Geophys. Res. Lett., 43, 10286-10294, https://doi.org/10.1002/2016gl070071, 2016.
Newcomb, C.J., Qafoku, N.P., Grate, J.W., Bailey, V.L., De Yoreo, J.J., Developing a molecular picture of soil organic matter–mineral interactions by quantifying organo–mineral binding. Nat. Commun., 8, 396, 2017.
Oades, J.M., The Retention of Organic-Matter in Soils. Biogeochem., 5, 35-70, https://doi.org/10.1007/Bf02180317, 1988.
Ontl, T.A., Schulte, L.A., Soil carbon storage. Nature Education Knowledge, 3, 2012.
Pansu, M., Gautheyrou, J., Handbook of soil analysis. Springer: Berlin, Germany, 2006.
Parfitt, R., Henmi, T., Comparison of an oxalate-extraction methon and an infrared spectroscopic method for determining allophane in soll clays. Soil Sci. Plant Nutr., 28, 183-190, 1982.
Parfitt, R.L., Allophane and imogolite: role in soil biogeochemical processes. Clay Miner., 44, 135-155, https://doi.org/10.1180/claymin.2009.044.1.135, 2009.
Parfitt, R.L., Childs, C.W., Estimation of Forms of Fe and Al - a Review, and Analysis of Contrasting Soils by Dissolution and Mossbauer Methods. Aust. J. Soil Res., 26, 121-144, https://doi.org/10.1071/Sr9880121, 1988.
Parfitt, R.L., Parshotam, A., Salt, G.J., Carbon turnover in two soils with contrasting mineralogy under long-term maize and pasture. Aust. J. Soil Res., 40, 127-136, https://doi.org/10.1071/Sr00105, 2002.

https://doi.org/10.5194/egusphere-2026-2843
Preprint. Discussion started: 25 August 2026

Paterson, E., Clark, L., Birnie, A.C., Sequential Selective Dissolution of Iron, Aluminum, and Silicon from Soils. Commun. Soil Sci. Plant Anal., 24, 2015-2023, https://doi.org/10.1080/00103629309368933, 1993.
Paul, E.A., The nature and dynamics of soil organic matter: Plant inputs, microbial transformations, and organic matter stabilization. Soil Biol. Biochem., 98, 109-126, 2016.
Percival, H.J., Parfitt, R.L., Scott, N.A., Factors controlling soil carbon levels in New Zealand grasslands is clay content important? Soil Sci. Soc. Am. J., 64, 1623-1630, 2000.
Pokrovski, G.S., Schott, J., Garges, F., Hazemann, J.L., Iron (III)-silica interactions in aqueous solution: Insights from X-ray absorption fine structure spectroscopy. Geochim. Cosmochim. Acta, 67, 3559-3573, https://doi.org/10.1016/S0016-7037(03)00160-1, 2003.
Rasmussen, C., Heckman, K., Wieder, W.R., Keiluweit, M., Lawrence, C.R., Berhe, A.A., Blankinship, J.C., Crow, S.E., Druhan, J.L., Pries, C.E.H., Marin-Spiotta, E., Plante, A.F., Schädel, C., Schimel, J.P., Sierra, C.A., Thompson, A., Wagai, R., Beyond clay: towards an improved set of variables for predicting soil organic matter content. Biogeochem., 137, 297-306, https://doi.org/10.1007/s10533-018-0424-3, 2018.
Rasmussen, C., Southard, R.J., Horwath, W.R., Mineral control of organic carbon mineralization in a range of temperate conifer forest soils. Glob. Chang. Biol., 12, 834-847, https://doi.org/10.1111/j.1365-2486.2006.01132.x, 2006.
Rayment, G.E., Lyons, D.J., Soil chemical methods: Australasia. CSIRO publishing, 2011.
Rennert, T., Wet-chemical extractions to characterise pedogenic Al and Fe species - a critical review. Soil Res, 57, 1-16, https://doi.org/10.1071/Sr18299, 2019.
Rennert, T., Händel, M., Höschen, C., Lugmeier, J., Steffens, M., Totsche, K.U., A NanoSIMS study on the distribution of soil organic matter, iron and manganese in a nodule from a Stagnosol. Eur. J. Soil Sci., 65, 684-692, https://doi.org/10.1111/ejss.12157, 2014.
Rennert, T., Lenhardt, K.R., Potential pitfalls when using popular chemical extractions to characterize Al- and Fe-containing soil constituents. J. Plant Nutr. Soil Sci., 188, 730-741, https://doi.org/10.1002/jpln.202300268, 2025.
Rezapour, S., Azhah, H., Momtaz, H.R., Ghaemian, N., Changes in forms and distribution pattern of soil iron oxides due to long-term cropping in the Northwest of Iran. Environ. Earth Sci., 73, 7275-7286, https://doi.org/10.1007/s12665-014-3933-y, 2015.
Ross, G.J., Wang, C., Schuppli, P.A., Hydroxylamine and Ammonium Oxalate Solutions as Extractants for Iron and Aluminum from Soils. Soil Sci. Soc. Am. J., 49, 783-785, https://doi.org/10.2136/sssaj1985.03615995004900030051x, 1985.
Ruiz, F., Ferreira, T.O., Delghingaro, G.C., de Souza Júnior, V.S., Demattê, J.A., Otero, X.L., Evaluating Sodium Pyrophosphate Extraction to Probe Soil Organo-Mineral Interactions Across Contrasting Pedogenic Stages. Eur. J. Soil Sci., 77, e70330, https://doi.org/10.1111/ejss.70330, 2026.
Scheel, T., Dörfler, C., Kalbitz, K., Precipitation of dissolved organic matter by aluminum stabilizes carbon in acidic forest soils. Soil Sci. Soc. Am. J., 71, 64-74, https://doi.org/10.2136/sssaj2006.0111, 2007.
Scheinost, A.C., Singh, B., Metal oxides. In: Goss, M.J., Oliver, M. (Eds.), Encyclopedia of Soils in the Environment. Academic Press, Oxford, 135-148. https://doi.org/10.1016/b978-0-12-822974-3.00069-0, 2023.
Schuppli, P.A., Ross, G.J., Mckeague, J.A., The Effective Removal of Suspended Materials from Pyrophosphate Extracts of Soils from Tropical and Temperate Regions. Soil Sci. Soc. Am. J., 47, 1026-1032, https://doi.org/10.2136/sssaj1983.03615995004700050037x, 1983.
Schweizer, S.A., Mueller, C.W., Höschen, C., Ivanov, P., Kögel-Knabner, I., The role of clay content and mineral surface area for soil organic carbon storage in an arable toposequence. Biogeochem., 156, 401-420, https://doi.org/10.1007/s10533-021-00850-3, 2021.
Schwertmann, U., Differentiation of the iron oxides of the soil by extraction with ammonium oxalate solution. J. Plant Nutri., Fertil., Soil Sci., 105, 194-202, https://doi.org/10.1002/jpln.3591050303, 1964.
Schwertmann, U., Schulze, D.G., Murad, E., Identification of Ferrihydrite in Soils by Dissolution Kinetics, Differential X-Ray-Diffraction, and Mossbauer-Spectroscopy. Soil Sci. Soc. Am. J., 46, 869-875, https://doi.org/10.2136/sssaj1982.03615995004600040040x, 1982.

https://doi.org/10.5194/egusphere-2026-2843
Preprint. Discussion started: 25 August 2026

Shang, C., Zelazny, L.W., Selective dissolution techniques for mineral analysis of soils and sediments. *Methods of Soil Analysis Part 5—Mineralogical Methods*. Wiley, 5, 33-80. https://doi.org/10.2136/sssabookser5.5.c3, 2008.
Singh, B., Gilkes, R.J., Phosphorus Sorption in Relation to Soil Properties for the Major Soil Types of South-Western Australia. Australian J. Soil Res., 29, 603-618, https://doi.org/10.1071/Sr9910603, 1991.
Singh, B., Gilkes, R.J., Properties and Distribution of Iron-Oxides and Their Association with Minor Elements in the Soils of South-Western Australia. J. Soil Sci., 43, 77-98, https://doi.org/10.1111/j.1365-2389.1992.tb00121.x, 1992.
Singh, B., Sherman, D.M., Gilkes, R.J., Wells, M., Mosselmans, J.F.W., Structural chemistry of Fe, Mn, and Ni in synthetic hematites as determined by extended X-ray absorption fine structure spectroscopy. Clays Clay Miner., 48, 521-527, https://doi.org/10.1346/Ccmn.2000.0480504, 2000.
Singh, B., Sherman, D.M., Gilkes, R.J., Wells, M.A., Mosselmans, J.F.W., Incorporation of Cr, Mn and Ni into goethite (α-FeOOH): mechanism from extended X-ray absorption fine structure spectroscopy. Clay Miner., 37, 639-649, https://doi.org/10.1180/000985502374066, 2002.
Six, J., Conant, R.T., Paul, E.A., Paustian, K., Stabilization mechanisms of soil organic matter: Implications for C-saturation of soils. Plant and Soil, 241, 155-176, https://doi.org/10.1023/A:1016125726789, 2002.
Skjemstad, J.O., Bushby, H.V.A., Hansen, R.W., Extractable Fe in the Surface Horizons of a Range of Soils from Queensland. Aust. J. Soil Res., 28, 259-266, https://doi.org/10.1071/Sr9900259, 1990.
Sollins, P., Homann, P., Caldwell, B.A., Stabilization and destabilization of soil organic matter: Mechanisms and controls. Geoderma, 74, 65-105, https://doi.org/10.1016/S0016-7061(96)00036-5, 1996.
Song, X., Wang, P., Van Zwieten, L., Bolan, N., Wang, H., Li, X., Cheng, K., Yang, Y., Wang, M., Liu, T., Towards a better understanding of the role of Fe cycling in soil for carbon stabilization and degradation. Carbon Res., 1, 5, 2022.
Song, Z.L., Liu, C.Q., Müller, K., Yang, X.M., Wu, Y.T., Wang, H.L., Silicon regulation of soil organic carbon stabilization and its potential to mitigate climate change. Earth-Sci. Rev., 185, 463-475, https://doi.org/10.1016/j.earscirev.2018.06.020, 2018.
Sparks, D.L., Singh, B., Siebecker, M.G., Environmental soil chemistry. Elsevier, 2024.
Steffens, M., Rogge, D.M., Mueller, C.W., Hoschen, C., Lugmeier, J., Kolbl, A., Kogel-Knabner, I., Identification of Distinct Functional Microstructural Domains Controlling C Storage in Soil. Environ. Sci. Technol., 51, 12182-12189, https://doi.org/10.1021/acs.est.7b03715, 2017.
Stewart, C.E., Paustian, K., Conant, R.T., Plante, A.F., Six, J., Soil carbon saturation: concept, evidence and evaluation. Biogeochem., 86, 19-31, https://doi.org/10.1007/s10533-007-9140-0, 2007.
Stuckey, J.W., Goodwin, C., Wang, J., Kaplan, L.A., Vidal-Esquivel, P., Beebe, T.P., Jr., Sparks, D.L., Impacts of hydrous manganese oxide on the retention and lability of dissolved organic matter. Geochem. Trans., 19, 6, https://doi.org/10.1186/s12932-018-0051-x, 2018.
Takahashi, T., Dahlgren, R.A., Nature, properties and function of aluminum-humus complexes in volcanic soils. Geoderma, 263, 110-121, https://doi.org/10.1016/j.geoderma.2015.08.032, 2016.
Torn, M.S., Trumbore, S.E., Chadwick, O.A., Vitousek, P.M., Hendricks, D.M., Mineral control of soil organic carbon storage and turnover. Nat., 389, 170-173, https://doi.org/10.1038/38260, 1997.
Vance, G.F., Stevenson, F.J., Sikora, F.J., Environmental chemistry of aluminum–organic complexes. The environmental chemistry of aluminum. CRC Press, 169-220. 2020.
Viscarra Rossel, R., Bui, E., De Caritat, P., McKenzie, N., Mapping iron oxides and the color of Australian soil using visible–near-infrared reflectance spectra. J. Geophys. Res. Earth Surf., 115, 2010.
Voelz, J.L., Johnson, N.W., Chun, C.L., Arnold, W.A., Penn, R.L., Quantitative Dissolution of Environmentally Accessible Iron Residing in Iron-Rich Minerals: A Review. ACS Earth Space Chem., 3, 1371-1392, https://doi.org/10.1021/acsearthspacechem.9b00012, 2019.
von Fromm, S.F., Jungkunst, H.F., Amenkhienan, B., Hall, S.J., Georgiou, K., Pries, C.H., Montaño-López, F., Quesada, C.A., Rasmussen, C., Schrumpf, M., Singh, B., Thompson, A., Wagai, R., Fiedler, S., Moisture and soil depth govern relationships between soil organic carbon and oxalate-extractable metals at the global scale. Biogeochem., 168, 20, https://doi.org/10.1007/s10533-025-01208-9, 2025.

https://doi.org/10.5194/egusphere-2026-2843
Preprint. Discussion started: 25 August 2026

von Lützow, M., Kögel-Knabner, I., Ludwig, B., Matzner, E., Flessa, H., Ekschmitt, K., Guggenberger, G., Marschner, B., Kalbitz, K., Stabilization mechanisms of organic matter in four temperate soils: Development and application of a conceptual model. J. Plant Nutr. Soil, 171, 111-124, 2008.
Vos, C., Jaconi, A., Jacobs, A., Don, A., Hot regions of labile and stable soil organic carbon in Germany - Spatial variability and driving factors. Soil, 4, 153-167, https://doi.org/10.5194/soil-4-153-2018, 2018.
Wada, K., Allophane and imogolite. In: Dixon, J.B., Weed, S.B. (Eds.), Minerals in soil environments. Soil Sci. Soc. Am. Inc. (SSSA), Madison, Wisconsin, 1051-1087. 1989.
Wagai, R., Kajiura, M., Asano, M., Iron and aluminum association with microbially processed organic matter via meso-density aggregate formation across soils: organo-metallic glue hypothesis. Soil, 6, 597-627, 2020.
Wagai, R., Mayer, L.M., Sorptive stabilization of organic matter in soils by hydrous iron oxides. Geochim. Cosmochim. Acta, 71, 25-35, https://doi.org/10.1016/j.gca.2006.08.047, 2007.
Wagai, R., Mayer, L.M., Kitayama, K., Shirato, Y., Association of organic matter with iron and aluminum across a range of soils determined via selective dissolution techniques coupled with dissolved nitrogen analysis. Biogeochem., 112, 95-109, https://doi.org/10.1007/s10533-011-9652-5, 2013.
Walker, A.L., The Effects of Magnetite on Oxalate-Extractable and Dithionite-Extractable Iron. Soil Sci. Soc. Am. J., 47, 1022-1026, https://doi.org/10.2136/sssaj1983.03615995004700050036x, 1983.
Wang, Y., Wang, H., He, J.S., Feng, X., Iron-mediated soil carbon response to water-table decline in an alpine wetland. Nat Commun, 8, 15972, https://doi.org/10.1038/ncomms15972, 2017.
Weaver, R.M., Syers, J.K., Jackson, M.L., Determination of Silica in Citrate-Bicarbonate-Dithionite Extracts of Soils. Soil Sci. Soc. Am. Proceedings, 32, 497-&, https://doi.org/10.2136/sssaj1968.03615995003200040023x, 1968.
Wiriyakitnateekul, W., Suddhiprakarn, A., Kheuruenromne, I., Gilkes, R.J., Extractable iron and aluminium predict the P sorption capacity of Thai soils. Aust. J. Soil Res., 43, 757-766, https://doi.org/10.1071/Sr05026, 2005.
Wiseman, C.L.S., Püttmann, W., Interactions between mineral phases in the preservation of soil organic matter. *Geoderma,* **134**, 109-118, https://doi.org/10.1016/j.geoderma.2005.09.001, 2006.
Ye, C.L., Huang, W.J., Hall, S.J., Hu, S.J., Association of Organic Carbon With Reactive Iron Oxides Driven by Soil pH at the Global Scale. Global Biogeochem. Cy., 36, e2021GB007128, https://doi.org/10.1029/2021GB007128, 2022.
Yeasmin, S., Singh, B., Johnston, C.T., Sparks, D.L., Organic carbon characteristics in density fractions of soils with contrasting mineralogies. Geochim. Cosmochim. Acta, 218, 215-236, https://doi.org/10.1016/j.gca.2017.09.007, 2017.
Yeasmin, S., Singh, B., Kookana, R.S., Farrell, M., Sparks, D.L., Johnston, C.T., Influence of mineral characteristics on the retention of low molecular weight organic compounds: a batch sorption-desorption and ATR-FTIR study. J. Colloid Interface Sci., 432, 246-257, https://doi.org/10.1016/j.jcis.2014.06.036, 2014.
Yu, M.X., Wang, Y.P., Jiang, J., Cao, N.N., Chang, Z.B., Zhang, S., Yan, J.H., Soil Organic Carbon Stabilization Is Dominated by Non-Sorptive Process Among the Subsoils From Different Parent Material. J. Geophys. Res. Biogeosci., 128, e2022JG007286, https://doi.org/10.1029/2022JG007286, 2023.
Yu, M.X., Wang, Y.P., Jiang, J., Wang, C., Zhou, G.Y., Yan, J.H., Soil Organic Carbon Stabilization in the Three Subtropical Forests: Importance of Clay and Metal Oxides. J. Geophys. Res. Biogeosci., 124, 2976-2990, https://doi.org/10.1029/2018jg004995, 2019.
Yu, W.J., Weintraub, S.R., Hall, S.J., Climatic and Geochemical Controls on Soil Carbon at the Continental Scale: Interactions and Thresholds. Global Biogeochem. Cy., 35, e2020GB006781, https://doi.org/10.1029/2020GB006781, 2021.
Zhang, X.D., Song, Z.L., McGrouther, K., Li, J.W., Li, Z.M., Ru, N., Wang, H.L., The impact of different forest types on phytolith-occluded carbon accumulation in subtropical forest soils. J. Soils Sediments, 16, 461-466, https://doi.org/10.1007/s11368-015-1259-3, 2016.

https://doi.org/10.5194/egusphere-2026-2843
Preprint. Discussion started: 25 August 2026

1178 Zhao, B., Dou, A., Zhang, Z.W., Chen, Z.Y., Sun, W.B., Feng, Y.L., Wang, X.J., Wang, Q., Ecosystem-specific
1179 patterns and drivers of global reactive iron mineral-associated organic carbon. Biogeosci., 20, 4761-4774,
1180 https://doi.org/10.5194/bg-20-4761-2023, 2023.
1181 Zhao, Q., Poulson, S.R., Obrist, D., Sumaila, S., Dynes, J.J., McBeth, J.M., Yang, Y., Iron-bound organic
1182 carbon in forest soils: quantification and characterization. Biogeosci., 13, 4777-4788,
1183 https://doi.org/10.5194/bg-13-4777-2016, 2016.
1184 Zhao, Y., Xiang, W., Ma, M., Zhang, X., Bao, Z., Xie, S., Yan, S., The role of laccase in stabilization of soil
1185 organic matter by iron in various plant-dominated peatlands: degradation or sequestration? Plant Soil,
1186 443, 575-590, 2019.
1187 Zimmerman, A.R., Chorover, J., Goyne, K.W., Brantley, S.L., Protection of mesopore-adsorbed organic
1188 matter from enzymatic degradation. Environ. Sci. Technol., 38, 4542-4548,
1189 https://doi.org/10.1021/es035340+, 2004.